



doi:10.1016/S0016-7037(03)00372-7

Modeling aqueous ferrous iron chemistry at low temperatures with application to Mars

GILES M. MARION,^{1,*} DAVID C. CATLING,² and JEFFREY S. KARGEL³¹Desert Research Institute, Reno, Nevada 89512, USA²University of Washington, Seattle, Washington 98195, USA³U.S. Geological Survey, Flagstaff, Arizona 86001, USA

(Received July 16, 2002; accepted in revised form May 15, 2003)

Abstract—Major uncertainties exist with respect to the aqueous geochemical evolution of the Martian surface. Considering the prevailing cryogenic climates and the abundance of salts and iron minerals on Mars, any attempt at comprehensive modeling of Martian aqueous chemistry should include iron chemistry and be valid at low temperatures and high solution concentrations. The objectives of this paper were to (1) estimate ferrous iron Pitzer-equation parameters and iron mineral solubility products at low temperatures (from < 0 °C to 25 °C), (2) incorporate these parameters and solubility products into the FREZCHEM model, and (3) use the model to simulate the surficial aqueous geochemical evolution of Mars.

Ferrous iron Pitzer-equation parameters were derived in this work or taken from the literature. Six new iron minerals [FeCl₂·4H₂O, FeCl₂·6H₂O, FeSO₄·H₂O, FeSO₄·7H₂O, FeCO₃, and Fe(OH)₃] were added to the FREZCHEM model bringing the total solid phases to 56. Agreement between model predictions and experimental data are fair to excellent for the ferrous systems: Fe-Cl, Fe-SO₄, Fe-HCO₃, H-Fe-Cl, and H-Fe-SO₄.

We quantified a conceptual model for the aqueous geochemical evolution of the Martian surface. The five stages of the conceptual model are: (1) carbonic acid weathering of primary ferromagnesian minerals to form an initial magnesium-iron-bicarbonate-rich solution; (2) evaporation and precipitation of carbonates, including siderite (FeCO₃), with evolution of the brine to a concentrated NaCl solution; (3) ferrous/ferric iron oxidation; (4) either evaporation or freezing of the brine to dryness; and (5) surface acidification.

What began as a dilute Mg-Fe-HCO₃ dominated leachate representing ferromagnesian weathering evolved into an Earth-like seawater composition dominated by NaCl, and finally into a hypersaline Mg-Na-SO₄-Cl brine. Weathering appears to have taken place initially under conditions that allowed solution of ferrous iron [low O₂(g)], but later caused oxidation of iron [high O₂(g)]. Surface acidification and/or sediment burial can account for the minor amounts of Martian surface carbonates. This model rests on a large number of assumptions and is therefore speculative. Nevertheless, the model is consistent with current understanding concerning surficial salts and minerals based on Martian meteorites, Mars lander data, and remotely-sensed spectral analyses. Copyright © 2003 Elsevier Ltd

1. INTRODUCTION

There are major uncertainties about the aqueous geochemical evolution of the Martian surface. For example, where are the surface carbonate sinks for the putative early CO₂ atmosphere? What is the solute composition of the Martian hydrosphere and precipitates formed from it, and how has composition evolved over time? What, if any, roles has low-temperature solution chemistry played in the alteration of Martian meteorites and Martian dust? What roles might solution chemistry have played in the development of the Martian hematite provinces and, more broadly, in the development of the red Martian surface? Direct evidence for the surface chemical composition comes principally from three sources: Martian meteorites, Mars landers, and remotely-sensed spectral analyses, including both Earth-based and Mars orbital observations.

Martian meteorites contain traces of water-precipitated minerals such as carbonates, sulfates, halides, ferric oxides, and aluminosilicate clays in a matrix dominated by ferromagnesian minerals (Gooding, 1992; McSween, 1994; Bridges and Grady, 2000; Bridges et al., 2001). Fe-Mg-Ca carbonates and gypsum

(CaSO₄·2H₂O) are common salts found in Martian meteorites; these minerals probably precipitated from saline solutions that were oxidizing and alkaline (Gooding, 1992; Bridges et al., 2001).

Both the Viking and Pathfinder landed missions have contributed to our understanding of Martian surface chemistry. On the basis of the Viking mission, Toulmin et al. (1977) concluded that the great preponderance of the material found in surficial fines on Mars have the overall composition suggestive of mafic rocks, which typically contain a high proportion of ferromagnesian minerals. Clark and Van Hart (1981) concluded that these surficial deposits must include a large salt component dominated by (Mg,Na)SO₄, NaCl, and (Mg,Ca)CO₃. A simple two-component model can explain all pair-wise trends in eight elements analyzed in the Viking landers (Clark, 1993); Component A (84%) contains Si and most or all the Al, Ca, Ti, and Fe (silicates, oxides); Component B (16%) contains S and most or all the Cl and Mg (salts). The Pathfinder mission found similar soil compositions to that found in the earlier Viking missions; but the analyzed rocks were similar to terrestrial andesites (Rieder et al., 1997; McSween and Murchie, 1999).

Remotely sensed spectral analyses have been used to place upper limits on dust and surface sulfates and carbonates on Mars (Blaney and McCord, 1989; Pollack et al., 1990; Chris-

* Author to whom correspondence should be addressed (gmarion@dri.edu).

tensen et al., 2000b). Calvin et al. (1994) presented spectroscopic evidence for the presence of hydrous carbonates on Mars. The Thermal Emission Spectrometer (TES) on the Mars Global Surveyor (MGS) has shown that the mineralogy of Martian dark materials is basaltic (composed of plagioclase feldspar, clinopyroxene, olivine, plus/minus sheet silicates) (Christensen et al., 2000b). Basalts occur primarily in the southern highlands, while andesites occur mostly in the younger northern plains. No globally extensive deposits having spectral characteristics resembling those of the Martian meteorites have been identified in TES data, which is puzzling (Christensen et al., 2000b). Similarly, TES indicates that deposits of $> \sim 5\%$ carbonates are not currently exposed at the Martian surface. TES recently found evidence of hematite deposits on Mars suggesting mineral precipitation from Fe-rich waters (Catling and Moore, 2000; Christensen et al., 2000a, 2001).

Some modelers have assumed that because the Earth and Mars supposedly had similar early environments (high CO_2 atmospheres, anoxic waters), early oceans or lakes on Earth and Mars would have had similar chemical compositions (e.g., Schaefer, 1990, 1993; Kempe and Kazmierczak, 1997; Morse and Marion, 1999). This assumption is consistent with Martian meteorite evidence that demonstrates the pervasiveness of carbonates and gypsum (Gooding, 1992), which are common minerals precipitating from terrestrial seawater (Marion and Farren, 1999). This assumption is, however, inconsistent with the landed missions, whose elemental abundance data are modeled in terms of a prevalence of MgSO_4 salts on Mars (Clark and Van Hart, 1981). This inconsistency has led some to argue that the MgSO_4 salts on the Martian surface are a relatively recent weathering product that involved volcanic acidic volatiles interacting with primary rock or secondary minerals (Settle, 1979; Clark and Van Hart, 1981; Banin et al., 1992, 1997; Clark, 1993).

Most attempts to model the surficial aqueous geochemistry of Mars have focused on an early, presumably warmer and wetter, Mars (e.g., Schaefer, 1990, 1993; Morse and Marion, 1999; Catling, 1999). For example, the FREZCHEM model was used to simulate an early alkaline Martian ocean (Morse and Marion, 1999). But this model did not contain iron chemistry, which made it impossible to quantify the role played by iron on the geochemical evolution of Mars. FREZCHEM uses the Pitzer approach for estimating solution activities and is valid across a broad range of solution compositions (dilute to concentrated brines) and temperatures (< -70 to 25°C) (Marion and Grant, 1994; Marion and Farren, 1999; Marion, 2001; Marion, 2002); these characteristics make this model highly relevant for cold Martian environments (Morse and Marion, 1999). The Catling model for Mars (Catling, 1999), on the other hand, dealt in detail with iron chemistry, but this model is only parameterized for 25°C . Any attempt to comprehensively model Martian aqueous chemistry must include iron chemistry and be valid at low temperatures and high solution concentrations.

The objectives of this paper were to (1) estimate ferrous iron Pitzer-equation parameters and iron mineral solubility products, (2) incorporate these parameters and solubility products into the FREZCHEM model, and (3) use the model to simulate aspects of the surficial aqueous geochemical evolution of Mars.

2. MATERIAL AND METHODS

2.1. Pitzer-Equation Parameterization

The osmotic coefficient of a solution and activity coefficients of chemical species in concentrated solutions can be estimated with the Pitzer equations, which have been presented in several recent papers (e.g., Harvie et al., 1984; Plummer et al., 1988; Spencer et al., 1990; Pitzer, 1991, 1995; Clegg et al., 1994; Marion and Farren, 1999). Therefore, this presentation will not be repeated here. To estimate the osmotic coefficient and ion activity coefficients using the Pitzer approach requires knowing the following interaction parameters: $\beta^{(0)}_{ca}$, $\beta^{(1)}_{ca}$, $\beta^{(2)}_{ca}$ (for divalent salts), C^{ϕ}_{ca} , $\Theta_{cc'}$ (or $\Theta_{aa'}$) and $\Psi_{cc'a}$ (or $\Psi_{caa'}$) for the appropriate solution phase ions, where c is a cation and a is an anion. Incorporation of carbonate chemistry into a model necessitates quantifying the activity coefficient of the neutral $\text{CO}_2(\text{aq})$ species in aqueous solutions. Similarly, incorporation of iron redox chemistry into a model necessitates quantifying the activity coefficient of the neutral $\text{O}_2(\text{aq})$ species in aqueous solutions. This is done with a Pitzer equation that is a function of $\lambda_{\text{CO}_2,c}$, $\lambda_{\text{CO}_2,a}$ and $\xi_{\text{CO}_2,c,a}$ interaction parameters and the O_2 analogues (Pitzer, 1991, 1995).

Pitzer-equation parameters and solubility products were estimated isothermally using a previously described algorithm (Marion and Farren, 1999). These isothermal constants were then fitted to equations of the form:

$$P(T)_j = a_{1j} + a_{2j}T + a_{3j}T^2 + a_{4j}T^3 + \frac{a_{5j}}{T} + a_{6j}\ln(T) + \frac{a_{7j}}{T^2} \quad (1)$$

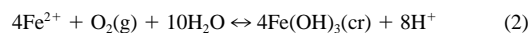
where P_j is the j^{th} Pitzer-equation parameter or Ln (solubility product) and T is temperature (K). The number of digits used in the data tables (e.g., Table 1) do not reflect the accuracy of the parameters, but only the number of digits needed to accurately reproduce the original parameters.

2.2. Iron Databases

The databases on iron mineral solubilities and freezing point depressions (fpd) for ferrous chemistry, FeCl_2 , FeSO_4 , $\text{FeCl}_2\text{-HCl}$, $\text{FeSO}_4\text{-H}_2\text{SO}_4$, were largely taken from the compilations of Linke (1958). The database used to quantify siderite (FeCO_3) solubility at 25°C was taken from Ptacek (1992). In many cases, necessary ferrous iron Pitzer-equation parameters have never been estimated. In these cases, the assumption was made to approximate the ferrous parameters by using the magnesium analogues (Reardon and Beckie, 1987; Ptacek, 1992; Ptacek and Blowes, 1994). Justification for this assumption will be discussed in the section on Limitations.

Pitzer-equation parameters for ferric ion interactions are largely unknown (Ptacek and Blowes, 2000). For this reason, a simplified chemistry was assumed to govern the ferrous-ferric iron transformations. No attempt was made to directly model the kinetics of the ferrous to ferric iron oxidation or the kinetics of ferric iron transformations. Our underlying assumption was that hematite (Fe_2O_3) forms through a series of more soluble intermediaries beginning with ferromagnesian minerals (Fig. 1). Ferrihydrite [$\text{Fe}(\text{OH})_3$] was chosen as the initial ferric precipitate because this mineral forms readily from aqueous solution (Lindsay, 1979) and is found in some Martian meteorites (Bridges et al., 2001). The model ignores the fact that initial $\text{Fe}(\text{OH})_3$ precipitates are likely to be amorphous with thermodynamic properties somewhat different than crystalline ferrihydrite (Lindsay, 1979; Nordstrom et al., 1990). We only attempted to model ferrihydrite precipitation and assumed that the subsequent reactions would proceed in good time. Judged from the iron minerals known or believed to occur on Mars (at least including iron-rich pyroxenes and olivine, siderite, ferrihydrite, goethite (FeOOH), magnetite (Fe_3O_4), and hematite), a large part of this reaction sequence (Fig. 1) appears to be represented on Mars (Gooding, 1992; Banin et al., 1992; Catling and Moore, 2000; Christensen et al., 2000a, 2001).

The governing equation for ferrihydrite formation is



where $\text{Fe}(\text{OH})_3(\text{cr})$ is ferrihydrite,

Table 1. Binary iron Pitzer-equation parameters derived in this work or taken from the literature. [Numbers are in computer scientific notation, where $e \pm xx$ stands for $10^{\pm xx}$].

| Pitzer-equation Parameter | Equation Parameter | | | | | | |
|------------------------------|--------------------|--------------|-------------|--------------|--------------|--------------|-------|
| | a_1 | a_2 | a_3 | a_4 | a_5 | a_6 | a_7 |
| $C_{Fe,Cl}^{\phi a}$ | -8.61e-3 | | | | | | |
| $B_{Fe,Cl}^{(0) a}$ | 3.359e-1 | | | | | | |
| $B_{Fe,Cl}^{(1) b}$ | 3.83836e1 | -1.236e-1 | | | | | |
| $C_{Fe,HCO_3}^{\phi c}$ | 0.0 | | | | | | |
| $B_{Fe,HCO_3}^{(0) c}$ | 1.369710e4 | 8.250840e0 | -4.34e-3 | | -2.7340617e5 | -2.6071152e3 | |
| $B_{Fe,HCO_3}^{(1) c}$ | -1.5783984e5 | -9.2777935e1 | 4.77642e-2 | | 3.2032097e6 | 2.9927152e4 | |
| $C_{Fe,SO_4}^{\phi d}$ | 2.09e-2 | | | | | | |
| $B_{Fe,SO_4}^{(0) d}$ | 1.29506e1 | -3.86e-2 | 3.91e-5 | | -1.38964e3 | | |
| $B_{Fe,SO_4}^{(1) b}$ | 8.758343e1 | -6.383194e-1 | 1.190408e-3 | | | | |
| $B_{Fe,SO_4}^{(2) d}$ | -4.20e1 | | | | | | |
| $C_{Fe,H_2SO_4}^{\phi d}$ | 0.0 | | | | | | |
| $B_{Fe,H_2SO_4}^{(0) b}$ | 6.758464e1 | -7.649696e-1 | 2.894494e-3 | -3.636364e-6 | | | |
| $B_{Fe,H_2SO_4}^{(1) d}$ | 3.48e0 | | | | | | |
| $C_{Fe,NO_3}^{\phi c}$ | -2.062e-2 | | | | | | |
| $B_{Fe,NO_3}^{(0) c}$ | 5.207e-1 | -5.1525e-4 | | | | | |
| $B_{Fe,NO_3}^{(1) c}$ | 2.9242e0 | -4.4925e-3 | | | | | |
| $C_{FeOH,Cl}^{\phi c}$ | 0.0 | | | | | | |
| $B_{FeOH,Cl}^{(0) c}$ | -1.0e-1 | | | | | | |
| $B_{FeOH,Cl}^{(1) c}$ | 1.658e0 | | | | | | |

^a Pitzer, 1991.

^b This work.

^c Assumed the same as the Mg analogues [Harvie et al., 1984 (MgOH-Cl); Marion, 2001 (Mg-HCO₃); Marion, 2002 (Mg-NO₃)].

^d Reardon and Beckie, 1987.

$$K = \frac{[Fe(OH)_3(cr)](H^+)^8}{(Fe^{2+})^4(O_2(g))(H_2O)^{10}} \quad (3)$$

The FREZCHEM model calculates H^+ , Fe^{2+} , and H_2O activities, which allows one to calculate the equilibrium $O_2(g)$ activity (Eqn. 3). The calculated $O_2(g)$ is compared to the model input of $O_2(g)$. If $O_2(g, calc.) > O_2(g, input)$, then the soluble iron is assumed to reside entirely in the ferrous state. Otherwise, if $O_2(g, calc.) \leq O_2(g, input)$, then the iron is assumed to reside entirely in the ferric state as ferrihydrite.

2.3. FREZCHEM Model

An objective of this work was to produce solubility products and Pitzer-equation parameters that can be incorporated seamlessly into the FREZCHEM model (Marion and Grant, 1994; Mironenko et al., 1997; Marion and Farren, 1999; Marion, 2001, 2002). The FREZCHEM model as presently structured has 56 solid phases including ice, 11 chloride minerals, 14 sulfate minerals, 15 carbonate minerals, five solid-phase acids, three nitrate minerals, six

acid-salts, and one iron oxide. For a listing of the previously defined solid phases (50), see Marion (2002); the six new minerals added in this work include $FeCl_2 \cdot 4H_2O$, $FeCl_2 \cdot 6H_2O$, $FeSO_4 \cdot H_2O$, $FeSO_4 \cdot 7H_2O$, $FeCO_3$, and $Fe(OH)_3$.

Solubility products for chloride minerals, the Debye-Hückel parameter, and 22 Pitzer-equation parameters dealing with chloride interactions were taken primarily from Spencer et al. (1990). Solubility products for sulfate minerals and 25 Pitzer-equation parameters dealing with sulfate interactions were taken primarily from Marion and Farren (1999). Solubility products for bicarbonate-carbonate minerals and 55 Pitzer-equation parameters dealing with bicarbonate, carbonate, and hydroxide interactions were taken primarily from Marion (2001). Solubility products for acids, nitrate minerals, and acid-salts and 82 Pitzer-equation parameters dealing with acid and nitrate interactions were taken primarily from Marion (2002). Solubility products for iron minerals and Pitzer-equation parameters dealing with ferrous iron interactions were estimated in this work.

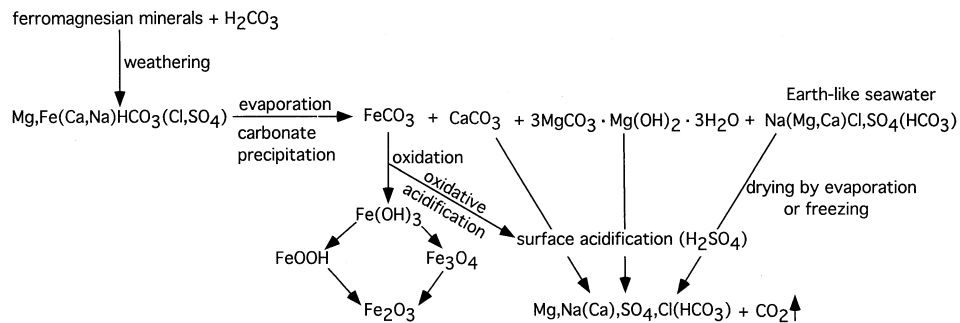


Fig. 1. A schematic of the evolution of surface Martian aqueous geochemistry. Major soluble salt components are unbracketed; minor soluble salt components are in parentheses.

Table 2. Equilibrium constants^a derived in this work or taken from the literature. [Numbers are in computer scientific notation, where e ± xx stands for 10^{±xx}].

| | Equation Parameters | | | | | | |
|---|---------------------|----------------|----------------|----------------|----------------|----------------|----------------|
| | a ₁ | a ₂ | a ₃ | a ₄ | a ₅ | a ₆ | a ₇ |
| Gas-Solution Phase Equilibria | | | | | | | |
| O ₂ (g) ↔ O ₂ (aq) ^b | 2.98399e-1 | | | | -5.59617e3 | | 1.049668e6 |
| 2H ₂ O(l) ↔ 2H ₂ (g) + O ₂ (g) ^c | 3.92869e1 | | | | -6.87562e4 | | |
| Solution Phase Equilibria | | | | | | | |
| Fe ²⁺ + H ₂ O ↔ FeOH ⁺ + H ⁺ ^c | 3.93e-1 | | | | -6.6392e3 | | |
| FeCO ₃ ⁰ ↔ Fe ²⁺ + CO ₃ ²⁻ ^c | -1.46641e1 | | | | 1.36517e3 | | |
| Solution-Solid Phase Equilibria | | | | | | | |
| FeCl ₂ · 4H ₂ O ↔ Fe ²⁺ + 2Cl ⁻ + 4H ₂ O ^{cd} | -4.594879e0 | 1.45731e-1 | -3.461353e-4 | | | | |
| FeCl ₂ · 6H ₂ O ↔ Fe ²⁺ + 2Cl ⁻ + 6H ₂ O ^c | -3.607762e2 | 4.61798e0 | -1.886403e-2 | 2.525105e-5 | | | |
| FeSO ₄ · H ₂ O ↔ Fe ²⁺ + SO ₄ ²⁻ + H ₂ O ^c | 6.324332e0 | -2.7915e-2 | | | | | |
| FeSO ₄ · 7H ₂ O ↔ Fe ²⁺ + SO ₄ ²⁻ + 7H ₂ O ^c | 2.096187e1 | -2.343349e-1 | 4.92807e-4 | | | | |
| FeCO ₃ ↔ Fe ²⁺ + CO ₃ ²⁻ ^c | -2.9654e1 | | | | 1.24845e3 | | |
| 4Fe ²⁺ + 10H ₂ O + O ₂ (g) ↔ 4Fe(OH) ₃ + 8H ⁺ ^c | -8.786e0 | | | | 1.04807e4 | | |

^a All equations in this table are presented as $\text{Ln}(K) = a_1 + a_2T + \dots$ (Eqn. 1).

^b Clegg and Brimblecombe, 1990.

^c This work.

^d This equation does not extrapolate well to temperatures below ≈ 263.15 K. Removed from model mineral database below 263.15 K.

3. RESULTS

3.1. FeCl₂ Chemistry

Binary Pitzer-equation parameters for Fe-Cl were based on published $\beta_{\text{Fe,Cl}}^{(0)}$, $\beta_{\text{Fe,Cl}}^{(1)}$, and $C_{\text{Fe,Cl}}^{\phi}$ at 25 °C (Pitzer, 1991) supplemented with freezing-point depression (fpd) data over the temperature range from -9 to -36.5 °C (Linke, 1958). The equation form used to estimate the temperature dependence was

$$P_T = P_{298.15} + k\Delta T \quad (4)$$

where P_T is the parameter value at temperature T , $P_{298.15}$ is the parameter value at 298.15 K, k is a derived constant, and ΔT is the difference in temperature (298.15- T). This equation form was eventually converted into that used in this work (Eqn. 1) before summarizing in tables. Neither $\beta_{\text{Fe,Cl}}^{(0)}$ nor $C_{\text{Fe,Cl}}^{\phi}$ showed a significant temperature dependence. In the final estimation, it was assumed that the “ k ” values for these two parameters were zero. The resulting Fe-Cl parameters are summarized in Table 1. Model values for $\beta_{\text{Fe,Cl}}^{(0)}$, $\beta_{\text{Fe,Cl}}^{(1)}$, and $C_{\text{Fe,Cl}}^{\phi}$ at 25 °C are 0.3359, 1.5323, and -0.00861, respectively, in reasonably good agreement with Pitzer (1991) values of 0.3363, 1.5133, and -0.0090, and with Ptacek (1992) values of 0.3621, 1.2699, and -0.0200, respectively. These binary Fe-Cl parameters were then used with FeCl₂ solubility data (Linke, 1958) to estimate solubility products for FeCl₂·4H₂O and FeCl₂·6H₂O (Table 2).

Overall, the fit of the model to fpd and mineral solubility data is good (Fig. 2). The model prediction for the eutectic, FeCl₂·6H₂O-Ice, occurs at a temperature of -36.9 °C with 3.44 m FeCl₂, in good agreement with literature values of -36.5 °C and 3.45 m FeCl₂ (Linke, 1958). The peritectic for the equilibrium, FeCl₂·4H₂O-FeCl₂·6H₂O, is modeled to occur at 12.1 °C with 4.73 m FeCl₂, in good agreement with literature values of 12.3 °C and 4.75 m FeCl₂ (Fig. 2), (Linke, 1958).

3.2. FeSO₄ Chemistry

Binary Pitzer-equation parameters for Fe-SO₄ and Fe-HSO₄ were taken from or derived from the equations of Reardon and Beckie (1987). The mathematical format of the latter study for $\beta_{\text{Fe,SO}_4}^{(0)}$ and $\beta_{\text{Fe,SO}_4}^{(1)}$ was changed to that used in this work (Eqn. 1). The equation for $\beta_{\text{Fe,SO}_4}^{(1)}$ was also extended to subzero temperatures based on five fpd data (Fig. 3). At 25 °C, the binary parameters for Fe-SO₄ and Fe-HSO₄ do not differ substantially from Reardon and Beckie (1987) or Ptacek and Blowes (1994). After the binary Fe-SO₄ parameters were incorporated into the model, a solubility product for FeSO₄·7H₂O (melanterite) was estimated from solubility data over the temperature range from -1.8 to 25 °C (Linke, 1958) (Table 2). At 25 °C, the calculated $\text{Ln}(K_{\text{sp}})$ is -5.098, in good agreement with $\text{Ln}(K_{\text{sp}}) = -5.086$ used by Reardon and Beckie (1987) and Ptacek and Blowes (1994).

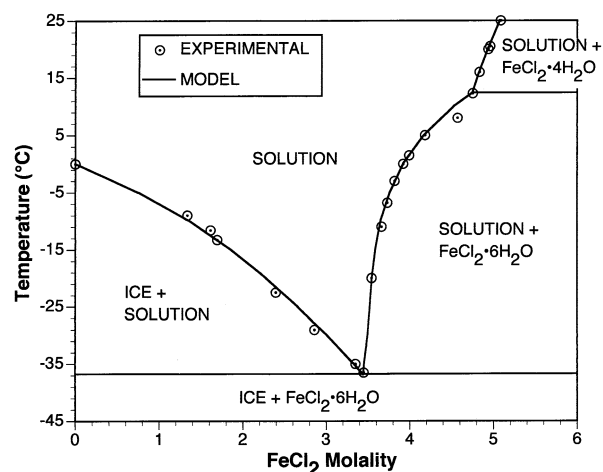


Fig. 2. Model and experimental estimates of equilibria for ferrous chloride solutions.

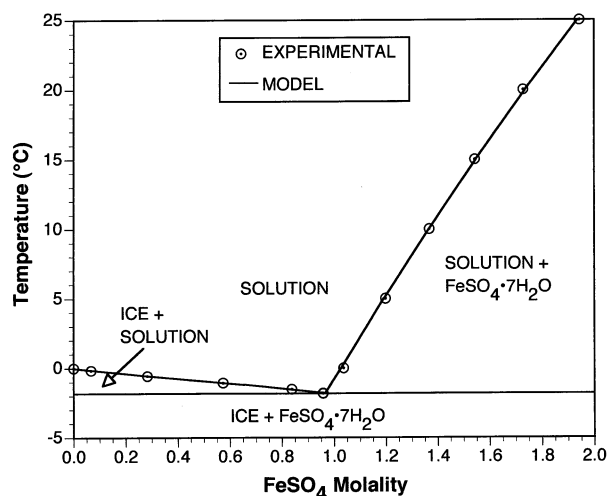


Fig. 3. Model and experimental estimates of equilibria for ferrous sulfate solutions.

The model provides an excellent fit to the fpd and solubility data (Fig. 3). The model calculated eutectic occurs at -1.8 °C with 0.969 m FeSO_4 . A literature value for this eutectic has a temperature of -1.8 °C with 0.957 m FeSO_4 (Linke, 1958). This fit is encouraging, since aqueous sulfate thermochemistry is highly nonideal.

3.3. FeCO_3 Chemistry

Siderite (FeCO_3) is an important mineral in many natural settings. The assumptions made to characterize this mineral and associated Pitzer-equation parameters closely followed Ptacek (1992). In the latter study, siderite solubility was measured at high ionic strengths and modeled using the Pitzer equations. In the latter study, where a critical property or parameter for $\text{Fe-HCO}_3\text{-CO}_3$ was unknown, the analogous $\text{Mg-HCO}_3\text{-CO}_3$ property or parameter was substituted.

To maintain consistency with previous versions of the FREZCHEM model, it was necessary to define equilibrium constants for two solution phase ion-associations, FeOH^+ and FeCO_3^0 . The temperature dependence of these two constituents was estimated by integrating the van't Hoff equation:

$$\frac{d\ln K}{dT} = \frac{\Delta H^0}{RT^2} \quad (5)$$

Assuming ΔH^0 is a constant, then integration yields

$$\ln K_T = \ln K_{298.15} + \frac{\Delta H^0}{R} \left(\frac{1}{298.15} - \frac{1}{T} \right) \quad (6)$$

which leads to equations of the form

$$\ln K_T = a_1 + \frac{a_5}{T} \quad (7)$$

(Table 2). For FeOH^+ , $\Delta H = 55.2$ kJ/mol and $\ln K_{298.15} = -21.875$ (Nordstrom et al., 1990). For FeCO_3^0 , $\Delta H = -11.351$ kJ/mol and $\ln K_{298.15} = -10.085$ (Nordstrom et al.,

1990). Because ΔH for FeCO_3^0 is unknown, we substituted the ΔH for MgCO_3^0 (Nordstrom et al., 1990).

The Fe-HCO_3 and FeOH-Cl binary interaction parameters were assumed to be the same as the Mg analogues (Table 1). Introduction of iron carbonate chemistry into the model necessitates describing Fe-CO_2 interactions. The three Pitzer-equation parameters for these interactions ($\lambda_{\text{CO}_2, \text{Fe}}$, $\xi_{\text{CO}_2, \text{Fe}, \text{Cl}}$, and $\xi_{\text{CO}_2, \text{Fe}, \text{SO}_4}$) were also assumed to be the same as the Mg analogues (Table 3).

A solubility product for siderite at 25 °C was estimated from the experimental database of Ptacek (1992). In the latter study, five experimental runs were made with variable molalities of NaCl and FeHCO_3 . There was good agreement in the calculated solubility product from the current work compared to Ptacek (1992) for four of the five runs (± 0.07 log units). For reasons not understood, Run 4 disagreed by 0.48 log units. For this reason, the latter data set was not used. There was also one run with variable Na_2SO_4 and FeHCO_3 molalities. The total number of datapoints used in estimating the siderite solubility product was 67 (55 NaCl and 12 Na_2SO_4).

The Pitzer-equation parameterization for $\text{Fe-HCO}_3\text{-CO}_3\text{-Cl-SO}_4$ led to a constant siderite solubility product independent of ionic strength and chemical composition (Fig. 4). The mean $\ln(K_{\text{FeCO}_3})$ was -25.467 , in good agreement with Ptacek's value of -25.494 for the same database. This good agreement is not surprising given that similar assumptions were made for the ferrous iron Pitzer-equation parameterization. These siderite equilibrium constants are slightly more insoluble than $\ln(K_{\text{FeCO}_3}) = -25.075$ recommended by Nordstrom et al., (1990). The consequences of this discrepancy for modeling Martian geochemistry will be discussed in the section of Limitations.

A temperature dependent equilibrium equation for siderite (Table 2) was estimated (Eqn. 6) by using $\ln(K_{\text{FeCO}_3}) = -25.467$ (this work) at 298.15 K and $\Delta H = -10.38$ kJ/mol (Nordstrom et al., 1990).

3.4. Iron Oxides

Incorporation of ferrous-ferric iron chemistry into the FREZCHEM model requires an explicit consideration of O_2 solubility because O_2 equilibrium frequently controls redox reactions in natural systems. The Pitzer-equation parameters (λ and ξ) for estimating the activity coefficient (γ) of the neutral $\text{O}_2(\text{aq})$ species were all taken from Clegg and Brimblecombe (1990) (Table 3). The Fe parameters were assumed to be the same as the Mg analogues (e.g., $\lambda_{\text{O}_2, \text{Fe}} = \lambda_{\text{O}_2, \text{Mg}}$).

The Henry's law constant for O_2 is given by

$$K_H = \frac{(\gamma_{\text{O}_2})(m_{\text{O}_2})}{P_{\text{O}_2}} \quad (8)$$

where γ_{O_2} is the activity coefficient, m_{O_2} is the molality of the aqueous O_2 species and P_{O_2} is the partial pressure of $\text{O}_2(\text{g})$. The mathematical equation used to quantify K_H was taken from Clegg and Brimblecombe (1990) (Table 2).

At a seawater salinity of 35.4 ‰, 24.8 °C, and $P_{\text{O}_2} = 0.203$ atm, the seawater O_2 concentration is calculated to be 214 μm , in excellent agreement with a measured seawater surface concentration of 214 μm at the same temperature and salinity

Table 3. A summary of the soluble gas Pitzer-equation parameters used in this work. All parameters in this table are from Clegg and Brimblecombe (1990) except for those that are footnoted. [Numbers are in computer scientific notation, where $e \pm xx$ stands for $10^{\pm xx}$].

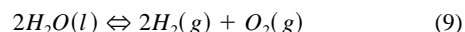
| Pitzer-equation Parameter | Equation Parameter | | | | | | |
|---|--------------------|-------------|-------------|---------------|----------------|-------|-----------|
| | a_1 | a_2 | a_3 | a_5 | a_6 | a_7 | |
| $\lambda_{\text{CO}_2, \text{Fe}}^a$ | -4.79362533e2 | -5.41843e-1 | 3.8812e-4 | 3.589474052e3 | 1.043452732e2 | | |
| $\lambda_{\text{O}_2, \text{Na}}$ | -3.9548e-1 | | 9.19882e-7 | 1.41307e2 | | | |
| $\lambda_{\text{O}_2, \text{K}}$ | -5.1698e-1 | | | 1.99431e2 | | | |
| $\lambda_{\text{O}_2, \text{H}}$ | -2.379e-1 | | | 8.1450e1 | | | |
| $\lambda_{\text{O}_2, \text{Mg}}^a$ | -7.9489e-1 | | | 3.05513e2 | | | |
| $\lambda_{\text{O}_2, \text{Fe}}^a$ | -7.9489e-1 | | | 3.05513e2 | | | |
| $\lambda_{\text{O}_2, \text{Ca}}$ | 2.497e-1 | | | | | | |
| $\lambda_{\text{O}_2, \text{Cl}}$ | 0.0 | | | | | | |
| $\lambda_{\text{O}_2, \text{OH}}$ | 9.3318e-1 | | | -4.30552e2 | | | 4.98608e4 |
| $\lambda_{\text{O}_2, \text{NO}_3}$ | -3.77e-2 | | | | | | |
| $\lambda_{\text{O}_2, \text{HCO}_3}$ | 8.54e-2 | | | | | | |
| $\lambda_{\text{O}_2, \text{CO}_3}$ | 1.0258e0 | | | -2.77074e2 | | | |
| $\lambda_{\text{O}_2, \text{SO}_4}$ | 1.00706e0 | | | -2.74085e2 | | | |
| $\xi_{\text{CO}_2, \text{Fe}, \text{Cl}}^a$ | -1.34260256e3 | -7.72286e-1 | 3.91603e-4 | 2.772680974e4 | 2.5362319406e2 | | |
| $\xi_{\text{CO}_2, \text{Fe}, \text{SO}_4}^a$ | -7.37424392e3 | -4.608331e0 | 2.489207e-3 | 1.431626076e5 | 1.412302898e3 | | |
| $\xi_{\text{O}_2, \text{Na}, \text{Cl}}$ | | | | -2.739e0 | | | |
| $\xi_{\text{O}_2, \text{Na}, \text{OH}}$ | -1.25e-2 | | | | | | |
| $\xi_{\text{O}_2, \text{Na}, \text{NO}_3}$ | -1.20e-2 | | | | | | |
| $\xi_{\text{O}_2, \text{Na}, \text{HCO}_3}$ | 0.0 | | | | | | |
| $\xi_{\text{O}_2, \text{Na}, \text{CO}_3}$ | -1.81e-2 | | | | | | |
| $\xi_{\text{O}_2, \text{Na}, \text{SO}_4}$ | -4.60e-2 | | | | | | |
| $\xi_{\text{O}_2, \text{K}, \text{Cl}}$ | -2.11e-2 | | | | | | |
| $\xi_{\text{O}_2, \text{K}, \text{OH}}$ | 2.342e-3 | | | | | | -8.3615e2 |
| $\xi_{\text{O}_2, \text{K}, \text{NO}_3}$ | -2.81e-2 | | | | | | |
| $\xi_{\text{O}_2, \text{K}, \text{SO}_4}$ | 0.0 | | | | | | |
| $\xi_{\text{O}_2, \text{Mg}, \text{Cl}}$ | -5.65e-3 | | | | | | |
| $\xi_{\text{O}_2, \text{Mg}, \text{SO}_4}$ | 0.0 | | | | | | |
| $\xi_{\text{O}_2, \text{Ca}, \text{Cl}}$ | -1.69e-2 | | | | | | |
| $\xi_{\text{O}_2, \text{Ca}, \text{NO}_3}$ | 0.0 | | | | | | |
| $\xi_{\text{O}_2, \text{Fe}, \text{Cl}}^a$ | -5.65e-3 | | | | | | |
| $\xi_{\text{O}_2, \text{Fe}, \text{SO}_4}^a$ | 0.0 | | | | | | |
| $\xi_{\text{O}_2, \text{H}, \text{Cl}}$ | -7.7e-3 | | | | | | |

^a Assumed the same as the Mg analogues (from Marion, 2001 or this work).

(Craig and Hayward, 1987). Similarly, at a seawater salinity of 33.7 ‰, 18.3 °C, and $P_{\text{O}_2} = 0.205$ atm, the seawater O_2 concentration is calculated to be 243 μm , again in good agree-

ment with a measured seawater surface concentration of 246 μm (Craig and Hayward, 1987). See Clegg and Brimblecombe (1990) for a thorough comparison of model and experimental O_2 solubilities.

In addition, we also estimated an equilibrium constant for the reaction



using the van't Hoff equation (Eqn. 6) with $\ln(K_{298.15}) = -191.3227$ and $\Delta H = 571.66$ kJ/mol (Drever, 1997)(Table 2). This equilibrium is used to estimate $\text{H}_2(g)$ from measured or calculated $\text{O}_2(g)$ and $\text{H}_2\text{O}(l)$ activities.

Eqn. 2 and 3 were assumed to govern the transformation from ferrous to ferric iron (see previous discussion). An equilibrium constant for this reaction was estimated using the van't Hoff equation (Eqn. 6) with $\ln(K_{298.15}) = 26.366$ (Drever, 1997) and $\Delta H = -87.14$ kJ/mol (Garrels and Christ, 1965) (Table 2). For a hypothetical case where $\text{Fe}^{2+} = 0.001$ m, $a_{\text{H}_2\text{O}} = 1.0$, and $a_{\text{Fe}(\text{OH})_3} = 1.0$, Eqn. 3 can be transformed to develop a stability diagram for ferrous and ferric iron. This relationship is not highly sensitive to temperature (Fig. 5). Ferrous iron is only stable at very low P_{O_2} and/or low pH. At the current Martian $\text{O}_2(g)$ concentration ($\approx 10^{-5}$ atm), ferrous iron is only stable at pH values less than 1.0 (Fig. 5), which is

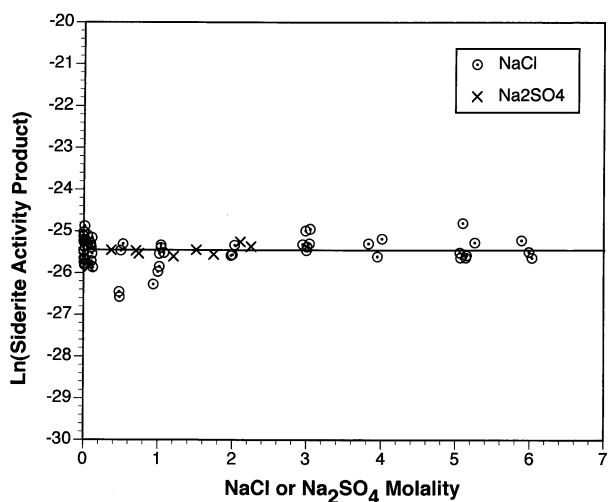


Fig. 4. Model estimates of siderite (FeCO_3) activity products as functions of background sodium chloride and sodium sulfate solutions.

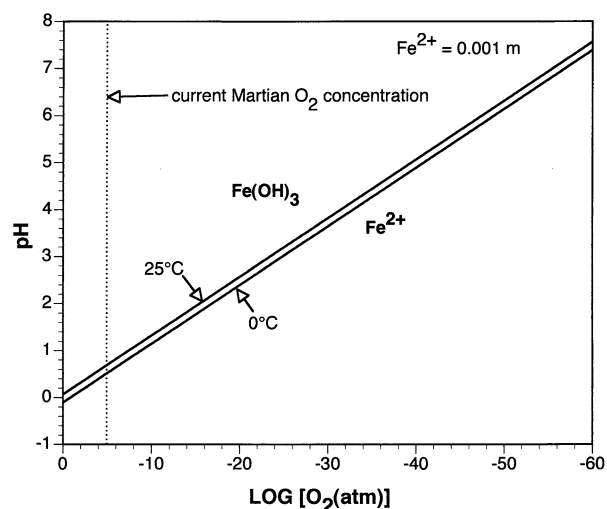


Fig. 5. A stability diagram for ferrous iron-ferrihydrite equilibrium as a function of pH and P_{O_2} .

probably why iron oxides are prevalent on the Martian surface (Toulmin et al., 1977; Burns, 1993; Rieder et al., 1997; Catling and Moore, 2000).

3.5. Ternary Iron Interactions

The ternary iron Pitzer-equation parameters used in this work are summarized in Table 4. Eleven of these parameters

were estimated by assuming the ferrous iron parameters are equal to the magnesium analogues. Four ternary Fe parameters were taken from the literature. Six parameters were estimated in this work. For example, because we assumed that Fe and Mg parameters should be similar, we assigned their interaction parameters ($\Theta_{Mg,Fe}$, $\Psi_{Mg,Fe,Cl}$, and Ψ_{Mg,Fe,SO_4}) values of zero (Table 4). The only other ternary Fe parameters estimated in this work were for the systems: HCl-FeCl₂-H₂O and H₂SO₄-FeSO₄-H₂O.

Two studies have measured the solubility of FeCl₂ salts in HCl at 0 and 20 °C (Schäfer, 1949; Schimmel, 1952); these experiments are summarized in Linke (1958). Given binary Fe-Cl parameters from this study (Table 1) and binary H-Cl parameters from a previous study (Marion, 2002), the only additional Pitzer-equation parameters needed to describe the HCl-FeCl₂-H₂O system are $\Theta_{H,Fe}$ and $\Psi_{H,Fe,Cl}$. Allowing both of these parameters to vary did not significantly improve the fit of the model to the experimental data compared to fixing $\Theta_{H,Fe}$ and only allowing $\Psi_{H,Fe,Cl}$ to vary. For this reason, we fixed $\Theta_{H,Fe}$ at 0.0 (Reardon and Beckie, 1987). The resulting fit of the model to the experimental data is only fair (Fig. 6). The model also misses the FeCl₂·4H₂O-FeCl₂·6H₂O equilibrium at 0 °C, which is modeled to occur at 7.79 m HCl and 0.83 m FeCl₂. An experimental measurement of this equilibrium places the composition at 6.49 m HCl and 1.23 m FeCl₂ (Linke, 1958).

Given binary parameters for Fe-SO₄ (Table 1) and binary parameters for H-SO₄ and H-HSO₄ (Marion, 2002), it is still necessary to consider $\Theta_{H,Fe}$, Ψ_{H,Fe,SO_4} , Ψ_{H,Fe,HSO_4} , $\Psi_{SO_4,HSO_4,Fe}$, C_{Fe,HSO_4}^ϕ , $\beta_{Fe,HSO_4}^{(0)}$, and $\beta_{Fe,HSO_4}^{(1)}$ to com-

Table 4. A summary of the iron ternary Pitzer-equation parameters used in this work. [Numbers are in computer scientific notation, where $e \pm xx$ stands for $10^{\pm xx}$].

| Pitzer-equation Parameter | Equation Parameter | | | | | |
|------------------------------|--------------------|---------------|-------------|--------------|---------------|--------------|
| | a_1 | a_2 | a_3 | a_4 | a_5 | a_6 |
| $\theta_{Na,Fe}^a$ | 8.0e-2 | | | | | |
| $\Psi_{Na,Fe,Cl}^a$ | -1.4e-2 | | | | | |
| Ψ_{Na,Fe,SO_4}^b | -1.207e-1 | 5.235e-4 | -5.39e-7 | -4.39e-10 | -1.723e1 | 1.2645e-2 |
| $\theta_{K,Fe}^b$ | 1.167e-1 | | | | | |
| $\Psi_{K,Fe,Cl}^b$ | 5.036223e-2 | -8.750820e-6 | | | -2.89909e1 | |
| Ψ_{K,Fe,SO_4}^b | -1.18e-1 | -4.78e-5 | -3.27e-7 | -9.37e-10 | 3.344e1 | -8.84e-3 |
| $\theta_{H,Fe}^c$ | 0.0 | | | | | |
| $\Psi_{H,Fe,Cl}^d$ | -1.4157e-1 | 5.15e-4 | | | | |
| Ψ_{H,Fe,SO_4}^b | 0.0 | | | | | |
| Ψ_{H,Fe,HSO_4}^d | 5.75716e1 | -5.7767e-1 | 1.924796e-3 | -2.129138e-6 | | |
| $\theta_{Mg,Fe}^d$ | 0.0 | | | | | |
| $\Psi_{Mg,Fe,Cl}^d$ | 0.0 | | | | | |
| Ψ_{Mg,Fe,SO_4}^d | 0.0 | | | | | |
| $\theta_{Ca,Fe}^b$ | 5.31274136e0 | -6.3424248e-3 | | | -9.83113847e2 | |
| $\Psi_{Ca,Fe,Cl}^b$ | 4.1579022e1 | 1.30377312e-2 | | | -9.81658526e2 | -7.4061986e0 |
| Ψ_{Ca,Fe,SO_4}^b | 2.4e-2 | | | | | |
| $\Psi_{Cl,SO_4,Fe}^b$ | 5.869e-2 | -8.97e-5 | 4.7e-8 | 6.5e-11 | -2.413e1 | 4.345e-3 |
| $\Psi_{Cl,HCO_3,Fe}^b$ | -9.6e-2 | | | | | |
| $\Psi_{SO_4,HCO_3,Fe}^b$ | -1.61e-1 | | | | | |
| $\Psi_{SO_4,HSO_4,Fe}^d$ | 0.0 | | | | | |
| $\Psi_{Fe,FeOH,Cl}^a$ | 2.8e-2 | | | | | |

^a Ptacek, 1992.

^b Assumed the same as the Mg analogues [Spencer et al., 1990 ($\theta_{Ca,Mg}$, $\theta_{K,Mg}$, $\Psi_{Ca,Mg,Cl}$, $\Psi_{K,Mg,Cl}$); Marion and Farren, 1999 (Ψ_{Na,Mg,SO_4} , Ψ_{K,Mg,SO_4} , Ψ_{Ca,Mg,SO_4} , $\Psi_{Cl,SO_4,Mg}$); Marion, 2001 ($\Psi_{Cl,HCO_3,Mg}$, $\Psi_{SO_4,HCO_3,Mg}$); Marion, 2002 (Ψ_{H,Mg,SO_4})].

^c Reardon and Beckie, 1986.

^d This work.

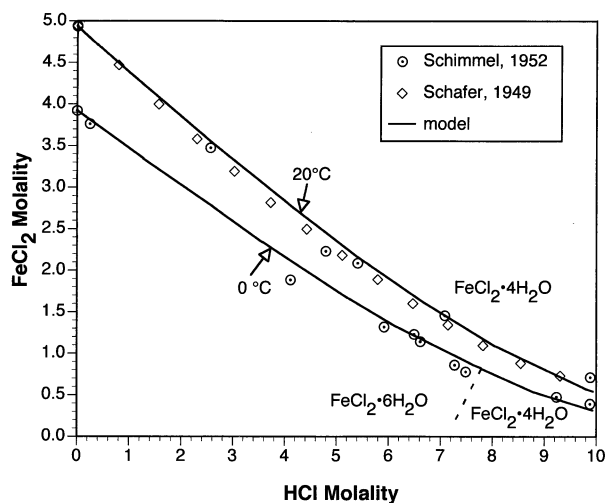


Fig. 6. Model and experimental estimates of equilibria for ferrous chloride-hydrochloric acid at 0 and 20 °C.

pletely describe the $\text{FeSO}_4\text{-H}_2\text{SO}_4\text{-H}_2\text{O}$ system. Fortunately many of these parameters are either redundant or known from previous work. In this paper, we assigned $\Theta_{\text{H,Fe}}$, $\Psi_{\text{H,Fe,SO}_4}$, $\Psi_{\text{SO}_4,\text{HSO}_4,\text{Fe}}$, and $C^{\phi}_{\text{Fe,HSO}_4}$ values of zero, and assigned $\beta^{(1)}_{\text{Fe,HSO}_4}$ a constant value of 3.48 (Reardon and Beckie, 1987) (Table 1 and 4). This only leaves $\Psi_{\text{H,Fe,HSO}_4}$ and $\beta^{(0)}_{\text{Fe,HSO}_4}$ undefined.

The latter parameters were estimated from $\text{FeSO}_4\text{-H}_2\text{SO}_4\text{-H}_2\text{O}$ data over the temperature range from -20 to 25 °C (Linke, 1958). The thermodynamic property used to estimate these parameters was the previously defined solubility product for $\text{FeSO}_4\cdot 7\text{H}_2\text{O}$ (Table 2). We estimated parameters that minimized the function

$$f = \sum [\ln(K_{sp}) - \ln(IAP)]^2 \quad (10)$$

where K_{sp} is the mineral solubility product and IAP is the ion activity product for a specific mineral, which can be calculated from measured molalities and the Pitzer equations for activity coefficients (Marion and Farren, 1999).

Once $\beta^{(0)}_{\text{Fe,HSO}_4}$ and $\Psi_{\text{H,Fe,HSO}_4}$ were known (Tables 1 and 4), we used the suite of binary and ternary $\text{Fe-H-SO}_4\text{-HSO}_4$ parameters to estimate a solubility product for $\text{FeSO}_4\cdot\text{H}_2\text{O}$ at 0 and 25 °C from solubility data (Linke, 1958)(Table 2).

The solubilities of FeSO_4 salts as a function of H_2SO_4 molality at 0 and 25 °C are shown in Figure 7. The fit again appears to be better at 0 °C than at 25 °C (cf., Figs. 6 and 7). The dip of the model 25 °C line below the 0 °C line at 7.5 m H_2SO_4 is an artifact of the model. The 0 and 25 °C experimental data do approach each other at H_2SO_4 molalities > 7.5 m. For example, the upper most data point in this region is a 25 °C point, while the two lower points are 0 °C data (Fig. 7). The calculated peritectic for $\text{FeSO}_4\cdot\text{H}_2\text{O}\text{-FeSO}_4\cdot 7\text{H}_2\text{O}$ at 25 °C is 1.05 m FeSO_4 and 5.37 m H_2SO_4 , compared to a literature value of 1.15 m FeSO_4 and 5.13 m H_2SO_4 (Linke, 1958). The calculated peritectic at 0 °C is 0.326 m FeSO_4 and 7.83 m H_2SO_4 , compared to a literature value of 0.323 m FeSO_4 and 7.81 m H_2SO_4 (Linke, 1958).

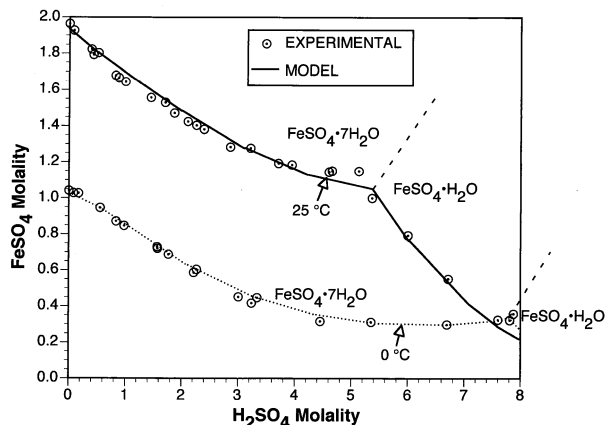


Fig. 7. Model and experimental estimates of equilibria for ferrous sulfate-sulfuric acid at 0 and 25 °C.

3.6. Summary of Results

What distinguishes the ferrous iron Pitzer-equation parameterization of this work from previous work (e.g., Reardon and Beckie, 1987; Ptacek, 1992; Ptacek and Blowes, 1994) is that we have extended the parameterizations into the subzero temperature range. For example, $\text{FeCl}_2\text{-H}_2\text{O}$ parameterization was extended to -36.5 °C (Fig. 2); $\text{FeSO}_4\text{-H}_2\text{O}$ parameterization was extended to -1.8 °C (Fig. 3); and $\text{FeSO}_4\text{-H}_2\text{SO}_4\text{-H}_2\text{O}$ parameterization was extended to -20 °C. This ferrous iron chemistry and O_2 chemistry were integrated into the FREZCHEM model, which is now parameterized for the $\text{Na-K-H-Mg-Ca-Fe-Cl-OH-NO}_3\text{-SO}_4\text{-HCO}_3\text{-CO}_3\text{-CO}_2\text{-O}_2\text{-H}_2\text{O}$ system [a FORTRAN version of this model is available from the senior author (GMM)]. This model enables us for the first time to examine ferrous iron chemistry at subzero temperatures on Earth and on other cold solar system bodies such as Mars and Europa.

4. VALIDATION

The paucity of ferrous iron data, especially of natural systems, makes it difficult to validate the model. While model fits to experimental data are encouraging (Figs. 2, 3, 4, 6, and 7), they are not validation, which requires comparison to independent data for multicomponent solutions. The only previously cited example where we compared the model to independent data was our comparison of O_2 solubility in seawater (see Section 3.4).

Bernard and Symonds (1989) reported solution concentrations on the bottom of Lake Nyos (-200 m) where siderite is forming in sediments due to high concentrations of CO_2 and Fe^{2+} (Table 5). Concentrations of Na^+ , K^+ , Mg^{2+} , Ca^{2+} , Fe^{2+} , Cl^- , SO_4^{2-} , alkalinity, and P_{CO_2} were used as input to the FREZCHEM model. Note the unusually high P_{CO_2} of 4.17 atm; this accounts for the occasional catastrophic CO_2 gas bursts from Lake Nyos (Bernard and Symonds, 1989). With this input and assuming no solid phases (pure solution phase model), the model predicts a carbonic acid concentration of 0.1485 m H_2CO_3 and a pH of 5.12 at equilibrium (Table 5). These values are in excellent agreement with model calculations of 0.1479 m H_2CO_3 and a pH of 5.13 made by Bernard

Table 5. The chemical composition of Lake Nyos water at -200 m (Bernard and Symonds, 1989).

| Element | Concentration |
|--|-----------------------|
| Na ⁺ (m) | 0.000776 |
| K ⁺ (m) | 0.000167 |
| Mg ²⁺ (m) | 0.00257 |
| Ca ²⁺ (m) | 0.000776 |
| Fe ²⁺ (m) | 0.000977 |
| Cl ⁻ (m) | 0.000017 |
| SO ₄ ²⁻ (m) | <0.000001 |
| Alkalinity (m) | 0.009572 ^a |
| P _{CO2} (atm) | 4.17 |
| H ₂ CO ₃ (m)(calc.) ^b | 0.1485 |
| pH (calc.) ^b | 5.12 |
| Ionic strength (m) | 0.0139 |
| Temperature (°C) | 23.3 |

^a Adjusted from 0.01 to 0.009572 m to give a perfect solution charge balance. This ignores the small contribution of Mn²⁺ (0.000025).

^b Calculated assuming a pure solution phase without minerals.

and Symonds (1989) using the SOLVEQ program (Reed, 1982; Reed and Spycher, 1984).

The FREZCHEM model predicts that this solution (Table 5) is supersaturated with siderite and no other carbonates, which agrees with Bernard and Symonds (1989). Allowing the solution to equilibrate with siderite causes the calculated pH to drop from 5.12 to 5.06 due to a small reduction in solution alkalinity as siderite precipitates.

5. APPLICATION TO MARS

As an example of how the newly iron parameterized FREZCHEM model can be used, we simulated the geochemical evolution of the Martian surface. Our understanding of past Martian climates, atmospheres, and geology is poorly constrained. As a consequence, these simulations are based on a large number of assumptions, which makes the proposed model somewhat subjective and speculative. Nevertheless, as we will show, the resulting model is consistent with current understanding concerning surficial salts and minerals based on Martian meteorites, Mars lander data, and remotely-sensed spectral analyses.

5.1. Background Assumptions

In using the FREZCHEM model to simulate Martian geochemistry, we removed magnesite (MgCO₃) and dolomite [CaMg(CO₃)₂] from the minerals database because these minerals do not easily precipitate at low temperatures despite their thermodynamic stability (Langmuir, 1964, 1965; Drever, 1997; Königsberger et al., 1999). This leaves hydromagnesite (3MgCO₃·Mg(OH)₂·3H₂O) as the most likely magnesium carbonate mineral to precipitate (Catling, 1999; Morse and Marion, 1999; Marion, 2001).

An underlying assumption in our conceptual model is that early Mars was warmer and wetter than present-day Mars due to high levels of atmospheric CO₂ that served as a greenhouse blanket (McKay and Stoker, 1989; Schaefer, 1990, 1993; Carr, 1996; Kargel and Strom, 1996; Zent, 1996; Forget and Pierrehumbert, 1997; Kempe and Kazmierczak, 1997; Haberle, 1998;

Kerr, 2000). Modern-day subsurface brine chemistry in geothermally heated groundwater zones is not modeled here, because key constraints due to the atmospheric CO₂ buffer and effects due to elevated pressures are not included in the present model. We also assumed that the surface geochemistry of Mars is primarily due to surface processes and ignored subsurface flows and processes. In what follows, we largely ignored temperature change as the CO₂ levels declined, and for simplicity ran most of the simulations at 0 °C. For a fuller discussion of declining CO₂ levels, accompanying temperature change, and freezing, see Morse and Marion (1999). We also treated evaporative concentration of solutions and loss of atmospheric CO₂, sequentially, realizing that, in fact, these two processes are occurring simultaneously.

In the simulations, we used the “equilibrium crystallization” option of the FREZCHEM model. This option allows a mineral that has precipitated to subsequently dissolve and reprecipitate as a different mineral along closed-system reaction pathways such as evaporation or temperature change. Under the equilibrium crystallization option, the final state of the system is independent of the pathway. For example, treating the aforementioned evaporation and loss of atmospheric CO₂ processes sequentially or simultaneously is irrelevant using equilibrium crystallization; both approaches lead to exactly the same final state. Under the alternative option of “fractional crystallization,” minerals that have precipitated are not allowed to dissolve and reprecipitate. Under this option, the pathway clearly affects the final state.

5.2. The Conceptual Model

In this paper, we quantified a conceptual model for the surficial aqueous geochemical evolution of Mars. This model rests on a foundation of previous work (e.g., Clark and Van Hart, 1981; Schaefer, 1990, 1993; Burns, 1993; Banin et al., 1997; Catling, 1999; Morse and Marion, 1999; Bridges and Grady, 2000; Catling and Moore, 2000; Bridges et al., 2001). With the incorporation of iron chemistry into the FREZCHEM model, we now have the capability to quantify the major low-temperature aqueous chemistries of Mars with the exception of silicon chemistry, which will be discussed under Limitations. The five stages of the conceptual model are: (1) carbonic acid weathering of primary ferromagnesian minerals to form an initial magnesium-iron-bicarbonate-rich solution; (2) evaporation and precipitation of carbonates, including siderite, with evolution of the brine to a concentrated NaCl solution; (3) ferrous/ferric iron oxidation; (4) evaporation or freezing of the brine to dryness; and (5) surface acidification (Fig. 1).

5.3. Martian Simulations

For the highland crust of early Mars, a mafic to ultramafic character is expected based on Martian meteorites (Gooding, 1992; McSween, 1994) and fundamental geochemical considerations (Toulmin et al., 1977; Baird and Clark, 1981; Burns, 1993). These rock types are dominated by ferromagnesian minerals that weather to produce solutions dominated by Fe²⁺, Mg²⁺, Ca²⁺, K⁺, and Na⁺. Initial P_{CO2} was assumed to be 2 atm, which is sufficient for greenhouse warming to >273 K with a faint early sun (Forget and Pierrehumbert, 1997). Under

Table 6. Martian and comparative solution compositions in the geochemical evolution of Mars.

| Solution Constituent | A. Hypothetical early Mars water ^a | B. 1000-fold concentration of Soln. A | C. Soln. B at lowered P_{CO_2} | D. Terrestrial seawater ^b | E. Soln. C with 1.665 m H_2SO_4 | F. Hypothetical Mars brine ^c |
|----------------------|---|---------------------------------------|----------------------------------|--------------------------------------|-----------------------------------|---|
| Na^+ (m) | 0.0008 | 0.8068 | 0.8101 | 0.4870 | 0.8101 | 0.9108 |
| K^+ (m) | 0.00007 | 0.0706 | 0.0709 | 0.0106 | 0.0709 | 0.0599 |
| Mg^{2+} (m) | 0.001 | 0.3744 | 0.0821 | 0.0552 | 1.743 ^d | 1.743 |
| Ca^{2+} (m) | 0.0005 | 0.00068 | 0.0011 | 0.0103 | 0.0022 ^d | 0.0022 |
| Fe^{2+} (m) | 0.0008 | 0.00000151 | — ^e | — | — ^e | — |
| Cl^- (m) | 0.00065 | 0.6556 | 0.6582 | 0.5682 | 0.6582 | 0.5256 |
| SO_4^{2-} (m) | 0.00018 | 0.1815 | 0.1823 | 0.0294 | 1.847 | 1.958 |
| Alkalinity (m) | 0.00446 | 0.6090 | 0.0246 | 0.00143 | 0.0184 | 0.0184 |
| P_{CO_2} (atm) | 2 | 2 | 0.0053 | 0.00035 | 0.0053 | 0.0053 |
| pH (calculated) | 5.00 | 6.84 | 8.03 | 8.05 | 7.57 | 7.58 |
| Ionic strength (m) | 0.008 | 2.19 | 1.31 | 0.723 | 7.95 | 8.17 |
| Temperature (°C) | 0 °C | 0 °C | 0 °C | 0 °C | 0 °C | 0 °C |

^a Catling, 1999.

^b Marion and Farren, 1999. This analysis assumes equilibrium with respect to calcite at 0 °C with $P_{CO_2} = 3.5 \times 10^{-4}$ atm (current Earth concentration).

^c Clark and Van Hart, 1981. Their Table III equilibrated at 0 °C.

^d Assumes that sufficient H_2SO_4 is added to solubilize Mg and Ca salts to match Soln. F.

^e At this stage and beyond, the assumption is made that all Fe would be irreversibly precipitated as a ferric mineral.

the high atmospheric CO_2 of early Mars, the dominant anion was probably bicarbonate. Therefore, based on Mars mineralogy and putative early high CO_2 levels, we used a hypothetical solution for early Mars water based on groundwater in terrestrial ultramafic rocks that is dominated by alkalinity (Catling, 1999) (Table 6, Soln. A). Note that this solution is similar in composition to the CO_2 - HCO_3^- water of Lake Nyos, Cameroon (cf., Tables 5 and 6A). This is not surprising given that biotite, a ferromagnesian silicate, is a major constituent of the Lake Nyos sediment silt (Bernard and Symonds, 1989), and Lake Nyos is situated amidst mafic to ultramafic alkaline volcanic rocks (Lockwood and Rubin, 1989).

This hypothetical early Mars water was subjected to concen-

tration by evaporation; we tracked its evolution until evaporation increased solutes by 1000 fold (Soln. B, Table 6). Because of the dominance of carbonate alkalinity in this solution, first siderite, then calcite, and finally hydromagnesite are predicted to precipitate at 0 °C (Fig. 8). Because of the insolubility of siderite, very little of the original Fe^{2+} remains in solution after a 1000-fold concentration. This particular simulation assumed no $O_2(g)$. As we demonstrated earlier, Fe^{2+} is unstable relative to Fe^{3+} minerals even at low levels of $O_2(g)$ (Fig. 5). The presence of hematite deposits on Mars—possible products of surface aqueous deposition (Catling and Moore, 2000; Christensen et al., 2000a, 2001)—and siderite in Martian meteorites (Clark and Van Hart, 1981; Gooding, 1992; Bridges et al.,

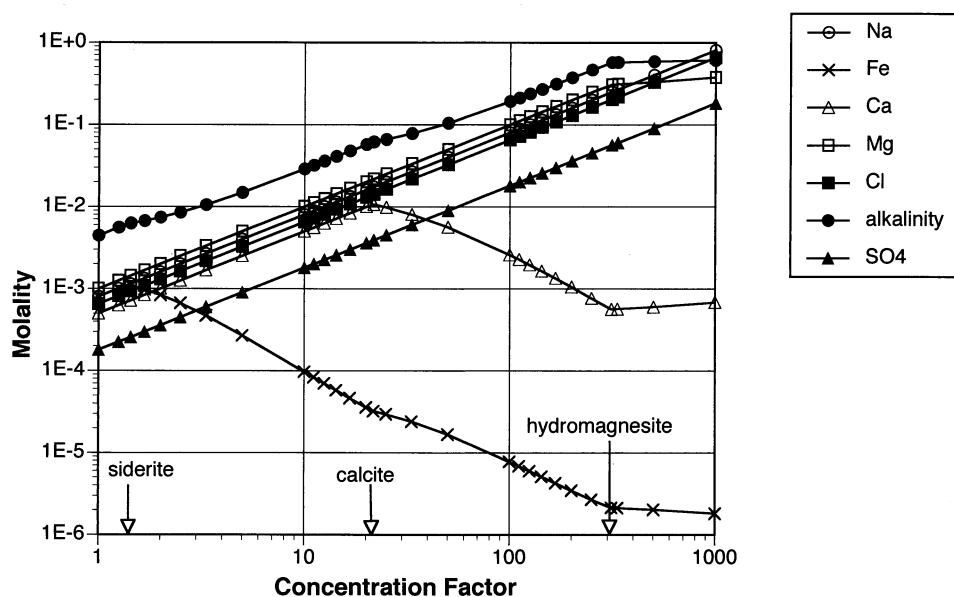


Fig. 8. A hypothetical early Mars water concentrated 1000-fold at 0 °C.

2001) suggests that there must have been times when environmental conditions were sufficiently reducing for high levels of ferrous iron to have existed. However, these periods were probably short-lived on Mars as they were on Earth (Burns, 1993; Catling and Moore, 2000), because equilibrium today on Mars exists well within the stability fields of ferric minerals (Fig. 5), as they do on Earth's surface. Today, iron oxides are the dominant form of surface iron on Mars (Toulmin et al., 1977; Burns, 1993; Banin et al., 1997; Rieder et al., 1997; Catling and Moore, 2000). The assumption was made based on this simulation that iron probably precipitated early in the geochemical evolution of Mars, perhaps first as the ferrous mineral, siderite, but ultimately oxidizing to ferric iron minerals; and once present as ferric iron, this oxidative transformation was probably irreversible (Fig. 1). In subsequent simulations, iron is assumed to be essentially absent because ferric iron compounds have a low solubility.

The evaporatively concentrated Mars water (Soln. B) was then allowed to drop in $\text{CO}_2(\text{g})$ concentration from 2 atm (the assumed initial Mars concentration) to 5.3×10^{-3} atm (the current average Mars concentration, Kieffer et al., 1992). This loss of CO_2 leads to a significant increase in pH from 6.84 to 8.03 and a significant additional precipitation of hydromagnesite; note the large drops in magnesium and alkalinity concentrations (cf., Soln. B and Soln. C, Table 6).

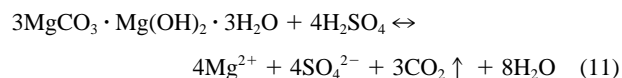
The resulting Soln. C is a predominantly NaCl solution similar to terrestrial seawater (Soln. D, Table 6). Had we chosen a concentration factor of 600-fold, the agreement would have been even better. In any case, the concentration factor is arbitrary. The point is that simple processes, starting with a dilute Fe-Mg- HCO_3 -rich solution formed by reaction of water with ultramafic and mafic rocks, evaporation, and carbonate precipitation, converted the solution into an Earth-like seawater NaCl brine. The Na/Mg ratio of solution C is 9.9, while terrestrial seawater has a Na/Mg ratio of 8.8 (Soln. D). Note also the similar pH values (8.03 and 8.05, Table 6). This solution did not (cannot) evolve into an alkali soda-lake composition as some have hypothesized or assumed for Mars (e.g., Kempe and Kazmierczak, 1997; Morse and Marion, 1999) because the mass of hypothesized soluble iron and magnesium and the low solubility of their respective carbonate minerals are sufficient to precipitate most of the initial soluble bicarbonate/carbonate ions.

The current surface of Mars is cold and dry. Early oceans or lakes would have dried out either by evaporation or freezing. Solution C was allowed to dry by either (a) evaporation at 0°C (Fig. 9A) or (b) freezing to the eutectic (Fig. 9B). Both equilibrium-mode evaporation and freezing lead to six precipitated salts (Fig. 9) because the number of independent salt components is equal to # of cations(4) + # of anions(3) - 1 = 6. The ensuing suite of minerals that theoretically precipitate are, however, different for these two scenarios. For example, drying by evaporation leads to precipitation of predominantly halite (NaCl), while freezing leads to predominantly hydrohalite ($\text{NaCl} \cdot 2\text{H}_2\text{O}$) (Figs. 9A-B). If states of mineral hydration are preserved in ocean or lacustrine deposits on Mars, then these records could provide valuable clues to the environmental history of Mars during the drying process.

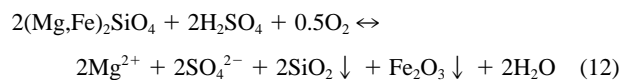
The last solid phase to precipitate during equilibrium-mode freeze-drying is $\text{MgSO}_4 \cdot 12\text{H}_2\text{O}$ at -35.4°C , which sets the

eutectic temperature. However, at this point, the solution is also nearing saturation with respect to $\text{MgCl}_2 \cdot 12\text{H}_2\text{O}$. If $\text{MgSO}_4 \cdot 12\text{H}_2\text{O}$ is dropped from the FREZCHEM minerals database, then $\text{MgCl}_2 \cdot 12\text{H}_2\text{O}$ begins precipitating at -36.3°C . The accuracies of the magnesium mineral solubility products at -36°C are not adequate to distinguish which of these two magnesium salts (chloride or sulfate) is the more likely.

If drying at this stage was the last step in the aqueous geochemical evolution of Mars, then we would expect to find surficial salts present in the order of abundance: $\text{NaCl} > (\text{MgNa})\text{SO}_4 > (\text{MgCa})\text{CO}_3$ (Figs. 9A-B). Instead we find surficial salts present in the order of abundance: $(\text{MgNa})\text{SO}_4 > \text{NaCl} > (\text{MgCa})\text{CO}_3$ (Clark and Van Hart (1981)). To reconcile this apparent discrepancy, we need to either add MgSO_4 or remove NaCl from the initial solution or at any step along the way. Past work suggests that acidification of the surface by volcanic acidic volatiles such as HCl, HNO_3 , or H_2SO_4 can explain the predominance of MgSO_4 salts on the surface of Mars (Settle, 1979; Clark and Van Hart, 1981; Clark, 1993; Banin et al., 1997). For example, addition of sulfuric acid to secondary hydromagnesite



would result in an increase in soluble magnesium and sulfate and a loss of CO_2 to the atmosphere. Or alternatively, sulfuric acid could react with primary ferromagnesian minerals



The net result is the same, an increase in MgSO_4 salts (Eqn. 11 and 12). Banin et al. (1997) have hypothesized that these volcanic acids are a relatively recent addition (up to 10^9 years B.P.).

Clark and Van Hart (1981) hypothesized that a Mg-Na- SO_4 brine from New Mexico (their Table III) is analogous to a Martian brine dominated by Mg-Na- SO_4 . Their brine was equilibrated at 0°C using the FREZCHEM model (Soln. F, Table 6) and was used in this study for comparative purposes.

We added sufficient sulfuric acid (1.665 m H_2SO_4) to the Martian seawater solution (Soln. C, Table 6) to increase the Mg and Ca molalities (Soln. E, Table 6) to those of the hypothetical Martian brine (Soln. F, Table 6). The assumption was made that for every 2 mol of added acidity, one mole of Mg or Ca and one mole of SO_4 were released into solution (Eqn. 11 and 12). As a consequence, the derived Soln. E and Soln. F agreed exactly in their Mg and Ca molalities (Table 6). Other constituents of our derived Soln. E, however, were not so constrained. Nevertheless, note the similar Na, K, Cl, SO_4 , alkalinity, pH values, and ionic strengths of Solns. E and F (Table 6). Note that the final brine composition (Soln. E, Table 6) has little carbonate alkalinity. By this stage, any significant surficial carbonates formed during the early geochemical evolution of Mars would either be buried by more soluble seawater salts and dust or removed by acidification. This may account for the minor amounts of carbonate found on the surface of Mars (Blaney and McCord, 1989; Pollack et al., 1990; Gooding, 1992; Calvin et

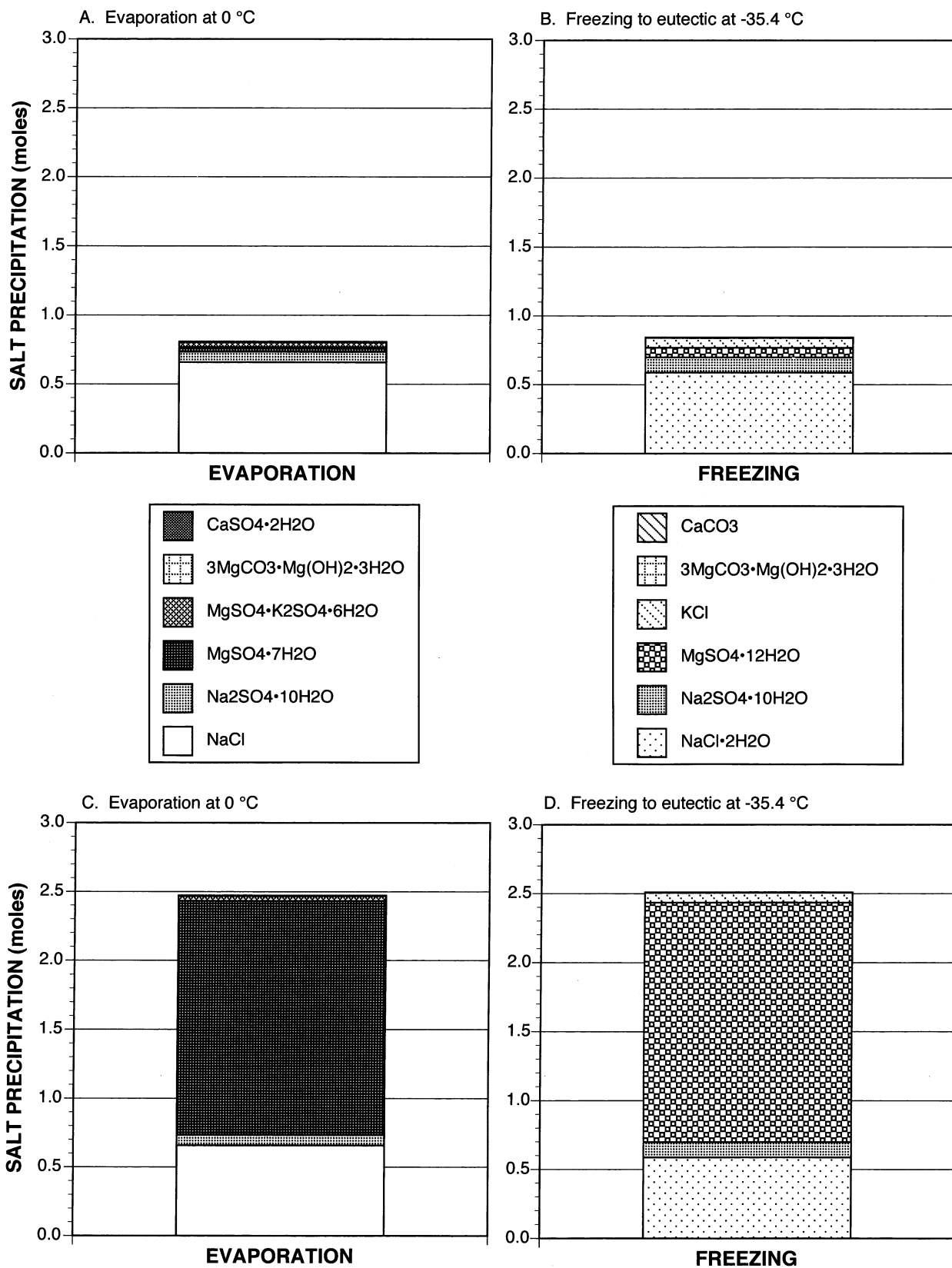


Fig. 9. Salt precipitation from Soln. C (Table 6) subjected to (A) evaporative drying at 0 °C and (B) freeze drying to the eutectic at -35.4 °C, and salt precipitation from Soln. E (Table 6) subjected to (C) evaporative drying at 0 °C and (D) freeze drying to the eutectic at -35.4 °C.

Table 7. A comparison of calculated Fe^{2+} , and CO_3^{2-} molal concentrations and activity coefficients, pH, and ionic strength with different assumptions for the siderite solubility product and binary Fe-HCO₃ Pitzer-equation parameters for Solution B (Table 6). [Numbers for Fe^{2+} are in computer scientific notation, where $e \pm xx$ stands for $10^{\pm xx}$].

| Case | [Fe ²⁺] | $\gamma_{\text{Fe}^{2+}}$ | [CO ₃ ²⁻] | $\gamma_{\text{CO}_3^{2-}}$ | pH | Ionic strength |
|--|---------------------|---------------------------|----------------------------------|-----------------------------|-------|----------------|
| Standard (Table 6) | 1.51e-6 | 0.1871 | 0.00136 | 0.0334 | 6.844 | 2.186 |
| With Nordstrom FeCO ₃ solubility product | 2.26e-6 | 0.1871 | 0.00136 | 0.0334 | 6.844 | 2.186 |
| With Fe-HCO ₃ binary parameters = 0.0 | 1.89e-6 | 0.1495 | 0.00136 | 0.0334 | 6.844 | 2.186 |
| With Nordstrom FeCO ₃ solubility product and Fe-HCO ₃ parameters = 0.0 | 2.81e-6 | 0.1495 | 0.00136 | 0.0334 | 6.844 | 2.186 |

al., 1994; Griffith and Shock, 1995; Christensen et al., 1998, 2000b).

In addition to acidification of the surface through volcanic acids, which we explicitly modeled (Table 6), there is another acidification process that is implicit in our model, but which was not explicitly considered: namely acidification resulting from oxidation of ferrous to ferric iron (Fig. 1). For every mole of iron that is oxidized, two moles of acid are produced (Eqn. 2). In terms of the original concentrations (Soln. A, Table 6), 0.0008 mol of Fe^{2+} would produce 0.0016 mol of H^+ . The amount of volcanic acid added (1.665 m H_2SO_4) in terms of the original concentrations (before the 1000-fold concentration) is equivalent to 0.00333 mol of H^+ . Together these two sources of acid add up to 0.00493 mol, which is more than enough to neutralize all the original alkalinity (0.00446 mol, Table 6). However, acids will also be neutralized by reaction with primary minerals (Eqn. 12). Based on the prevalence of carbonates, especially siderite, in Martian meteorites (Bridges et al., 2001), it is unlikely that acidification processes neutralized all the alkalinity on Mars or that all the ferrous iron was oxidized.

If Soln. E is allowed to dry by evaporation at 0 °C (Fig. 9C) or freezing to the eutectic (Fig. 9D), then the distribution of precipitated salts is similar to Soln. C except for the large increase in MgSO_4 salts (cf., Figs. 9A-B with 9C-D). Exactly the same suite of salts precipitate for Solns. C and E. Also, the eutectic temperature is the same (-35.4 °C). For Soln. E, the salt quantities fall in the order $(\text{MgNa})\text{SO}_4 > \text{NaCl} > (\text{Mg-Ca})\text{CO}_3$ in agreement with estimates of salt distribution on the Martian surface (Clark and Van Hart, 1981).

Figure 1 summarizes the evolution of the surface aqueous geochemistry of Mars. The process begins with the weathering of ferromagnesian minerals by carbonic acid leading to a predominantly Mg-Fe-HCO₃ solution. As this solution evaporates, iron, calcium, and magnesium carbonate minerals precipitate drawing down the atmospheric CO₂, which cools the surface temperature on Mars. The resulting solution has an Earth-like seawater composition (NaCl dominated). Ferrous iron is irreversibly oxidized to ferric minerals early in the geochemical evolution of Mars. Eventually, the seawater would dry either by evaporation or freezing. And finally the surface is acidified by volcanic volatile acids or ferrous iron oxidation producing a predominantly Mg-Na-SO₄-Cl salt phase. The precise timing of drying and acidification is uncertain. There is evidence for enormous floods throughout Martian history (Carr, 1996). Oceans/lakes were likely ephemeral, alternating forming and drying out. Banin et al. (1997) have hypothesized that volcanic acidification was a relatively recent phenomenon (up to 10⁹ years B.P.); on the other hand, oxidative acidification could have occurred early in Mars history whenever oxygen levels in the atmosphere became sufficiently high. The transformation

from a NaCl into a Mg-Na-SO₄-Cl brine via acidification could have been gradual with alternating wet and dry periods.

6. LIMITATIONS

6.1. Model Parameterization

The database for ferrous chemistry is rather limited (Linke, 1958). This is largely because ferrous iron is unstable relative to ferric iron at the prevailing level of atmospheric oxygen on Earth ($P_{\text{O}_2} \approx 0.203$ atm), and so less attention has been given to ferrous iron-bearing solutions, especially at low temperatures. In experimental work, special precautions are necessary to isolate ferrous chemistry from atmospheric oxygen.

One of the consequences of this limited database was the necessity to substitute, in several cases, magnesium analogues for unknown ferrous iron parameters or properties (Tables 1–4). In defining activity coefficients using the Pitzer approach, the most important iron parameters are the binaries ($\beta^{(0)}_{\text{ca}}$, $\beta^{(1)}_{\text{ca}}$, $\beta^{(2)}_{\text{ca}}$ (for divalent salts), and $C^{\text{cl}}_{\text{ca}}$) for Fe-Cl, Fe-SO₄, Fe-HSO₄, FeOH-Cl, Fe-NO₃, and Fe-HCO₃. Fortunately, from various literature databases and sources, we were able to directly estimate binaries for Fe-Cl, Fe-SO₄, and Fe-HSO₄ (Table 1). For the remaining three binaries, we made the magnesium for iron substitution. The FeOH-Cl, binaries describe a minor chemistry that was included in this work for completeness; it is likely that whether assumptions are made with respect to these parameters would only have a minor influence on defining solution properties. Examples will be described later in Table 7 that demonstrate the role of minor constituents on solution properties. The database on Fe-NO₃ properties only include limited solubility data at high concentrations (Linke, 1958), which is inadequate for accurately determining Pitzer parameters. Lack of “true” Fe-NO₃ parameters could potentially be a major problem in cases where both Fe^{2+} and NO_3^- are present at high concentrations, which is unlikely in most natural environments where the presence of oxygen, bicarbonate, and carbonate would keep Fe^{2+} concentrations at low levels. This leaves only the Fe-HCO₃ binary parameters as a major source of concern with respect to defining activity coefficients.

We made an effort to estimate binary Fe-HCO₃ Pitzer-equation parameters from the database of Ptacek (1992). In our work, we assumed a magnesium for iron substitution for the Fe-HCO₃ binaries and estimated a solubility product for siderite (Fig. 4). An alternative was to use a solubility product from the literature [e.g., $K = 1.288 \times 10^{-11}$ at 25 °C, Nordstrom et al., (1990)] and estimate Fe-HCO₃ binaries from the Ptacek (1992) database. However, this effort failed probably because the iron concentrations are very low (μm) compared to the NaCl (m), NaHCO₃ (mm), and Na₂SO₄ (m) background

salts. Our optimized estimates of $C_{\text{Fe,HCO}_3}^{\phi}$, $\beta_{\text{Fe,HCO}_3}^0$, and $\beta_{\text{Fe,HCO}_3}^1$ were -11.72 , 68.78 , and -52.08 , which are orders of magnitude off from “normal” values for similar chemistries (Pitzer, 1991, 1995).

Table 7 compares several options for calculating the properties of Soln. B (Table 6). The first example (Standard Case, Table 7) is our existing model. The second case uses the Nordstrom et al. (1990) solubility product for siderite ($K = 1.905 \times 10^{-11}$ at 0°C , calculated using Eqn. 6 and their values for K at 25°C and ΔH_p); our model, in contrast, uses a value of $K = 1.28 \times 10^{-11}$ at 0°C . In this second case, the solubility of Fe^{2+} increases in solution; but all other properties remain the same. In the third case, we assigned the three binary Fe-HCO₃ parameters values of 0.0; this causes a decrease in the activity coefficient of Fe^{2+} and a corresponding increase in the solubility of Fe^{2+} . The final case combines the two previous assumptions; in this case, the solubility of Fe^{2+} reaches a maximum (Table 7). A point of these different scenarios for defining iron chemistry is to demonstrate that because iron is a minor constituent, iron parameterization plays an insignificant role in defining the major properties of these aqueous solutions (e.g., CO_3^{2-} , pH, and ionic strength, Table 7). On the other hand, assumptions about iron parameterizations do directly affect iron solubilities. However, a 1000-fold concentration of Soln. A (Table 6) would cause anywhere from 99.96 to 99.98% of the iron to precipitate for the four examined cases in Table 7. The fact that there is a small difference in the residual solution concentrations is insignificant. Virtually all the iron would have precipitated regardless of the assumptions made in defining iron bicarbonate/carbonate chemistry.

And finally, there is direct evidence that the magnesium for iron substitution is reasonable. For example, at 25°C and 1.0 m, the model-calculated mean activity coefficients, a direct function of binary Pitzer-equation parameters, for FeCl_2 and MgCl_2 are 0.506 and 0.589, respectively. Similarly, at 25°C and 1.0 m, the mean activity coefficients for FeSO_4 and MgSO_4 are 0.0537 and 0.0545, respectively. Also, the calculated siderite solubility product is independent of salt concentrations across a broad range of concentrations (Fig. 4), which is further evidence that the magnesium for iron substitution is reasonable.

Some of our estimated temperature-dependent parameters were based on few temperatures. For example, our linear equation for $\Psi_{\text{H,Fe,Cl}}$ (Table 4) was only based on data at 0 and 20°C . On the other hand, our equations for $\beta_{\text{Fe,HSO}_4}^{(0)}$ and $\Psi_{\text{H,Fe,HSO}_4}$ (Tables 1 and 4) were based on six temperatures over a broader range (-20 to 25°C).

Even in cases where there were some ferrous iron data, estimating and applying iron Pitzer-equation parameters and iron solubility products can still be problematic. For example, we used solubility data for $\text{FeSO}_4 \cdot 7\text{H}_2\text{O}$ for the temperature range from -1.8 to 25°C to estimate a solubility product. This is adequate to describe pure FeSO_4 systems (Fig. 3). How well the linear $\text{FeSO}_4 \cdot 7\text{H}_2\text{O}$ solubility product equation (Table 2) would extrapolate to lower temperatures is an open question. An example from the simulations of this study will illustrate the inherent problem. In the freezing of the Martian seawater (Fig. 9B), we indicated that it was difficult to be sure that $\text{MgSO}_4 \cdot 12\text{H}_2\text{O}$ is more likely to precipitate at the eutectic rather than $\text{MgCl}_2 \cdot 12\text{H}_2\text{O}$. There is experimental data for pure $\text{MgCl}_2 \cdot 12\text{H}_2\text{O}$ solubility to the eutectic for $\text{MgCl}_2 \cdot 12\text{H}_2\text{O}$ -Ice

at -34°C , which was used in defining a solubility product for $\text{MgCl}_2 \cdot 12\text{H}_2\text{O}$ (Spencer et al., 1990). The coldest temperatures for $\text{MgSO}_4 \cdot 12\text{H}_2\text{O}$ solubility data is -8°C (Marion and Farnen, 1999). Our estimate that $\text{MgSO}_4 \cdot 12\text{H}_2\text{O}$ should precipitate at a eutectic of -35.4°C (Fig. 9B) involved a 27°C extrapolation of a linear equation beyond the range of the database. The accuracy of such an extrapolation is very uncertain, as also would be the case if we extrapolated the $\text{FeSO}_4 \cdot 7\text{H}_2\text{O}$ equation, similarly.

Application of this model to strongly acidic systems on Earth, such as acid mine drainage (AMD), would necessitate the incorporation of new chemistries into the model and consideration of transport processes. For example, there are many complex sulfate minerals that form in AMD (Alpers et al., 2000), which are not now part of the FREZCHEM model. Also for short-term simulations of ground-water flows, kinetics of reactions and transport processes would be important (Ptacek and Blowes, 1994).

6.2. Mars Application

An element notably absent from the FREZCHEM model that could have played a significant role in iron chemistry on Mars is silicon (Si). Weathering of ferromagnesian minerals (Fig. 1) will release silicon to the environment (Eqn. 12). Catling (1999) explicitly considered silicon chemistry in his model of Martian aqueous geochemistry. According to the Catling model, silicon should precipitate as silica (SiO_2) early (before siderite) in the evaporation of the hypothetical early Mars water (Soln. A, Table 6) at $P_{\text{CO}_2} = 2$ atm (see Fig. 2 in Catling, 1999). At P_{CO_2} values < 0.1 atm, amorphous greenalite [$\text{Fe}_3\text{Si}_2\text{O}_5(\text{OH})_4$] or ferrous smectite-type clays rather than silica are the most likely silicon sinks. If Mars evolved from a high (>1 atm) to a low (<0.1 atm) CO_2 environment, it is unlikely that greenalite or ferrous clays would have been important because by the time the CO_2 dropped into the stability zone for these minerals ($P_{\text{CO}_2} \approx 0.1$ atm), most of the silicon (as SiO_2) and iron (as FeCO_3 or iron oxide) would have precipitated (see Fig. 2 in Catling, 1999). On the other hand, if P_{CO_2} was always low, then minerals like greenalite and/or ferrous clays may have played a role in Martian iron chemistry.

There is abundant evidence for the presence of secondary aluminosilicate clay minerals in Martian meteorites and soils (Toulmin et al., 1977; Gooding, 1992; Burns, 1993; Clark, 1993; Banin et al., 1997). These clay minerals could be important sinks for either iron or magnesium. For example, Clark (1993) found that iron was principally associated with silicates in a two-component model of Martian soil (silicates + salts). However, this does not necessarily mean that the iron was directly bound within a silicate crystal structure; instead iron could be present as nanometer-sized grains of ferric oxide bound to the large surface area clays (Clark, 1993).

The model simulation assumes that early Mars was warmer and wetter with open bodies of water as the result of greenhouse warming by CO_2 . While this model of an early Mars is the current paradigm (Carr, 1996; Kargel and Strom, 1996; Zent, 1996; Head et al., 1998; Kerr, 2000), there are alternative models. For example, there is evidence that early Mars might have been colder and more Arctic-like (Newsom, 1996; Haberle, 1998; Gaidos and Marion, 2003); this perspective is

largely based on the inability of atmospheric CO₂, per se, to produce sufficient greenhouse warming (Kasting, 1991). Alternative mechanisms to assist CO₂ warming on early Mars such as reduced CH₄ and NH₃ gases (Sagan and Chyba, 1997) or the presence of CO₂ ice clouds (Forget and Pierrehumbert, 1997) may fix the “sufficient” warming problem, but the question is far from being resolved (Kasting, 1997; Haberle, 1998). If Mars never experienced significant periods of surface melting, chemical alteration and brine formation may have been predominantly a subsurface phenomenon. In that case, effects of elevated pressures (e.g., 500 bars at 5 km depth) and subsurface transport would have to be considered. For example, as an aqueous solution flows through subsurface layers, insoluble minerals first precipitate followed later by more soluble minerals. This leads to the continuous alteration of the aqueous solution and a chromatographic separation of solid phases, which requires a model with sound elemental accounting and transport mechanisms (Marion et al., 1985; Gaidos and Marion, 2003). On the other hand, in the model presented in this paper, we assumed that surface waters with compositions similar to Soln. A (Table 6) collected in basins; this was followed by evaporation and freezing that altered compositions. These surficial mechanisms lead to layering of minerals, with the most insoluble at the bottom and the most soluble at the surface of basins (e.g., see Fig. 7 in Catling, 1999).

Acknowledgments—Funding was provided by a NASA Planetary Geology and Geophysics Project, “An Aqueous Geochemical Model for Cold Planets,” and a NASA EPSCoR Project, “Building Expertise and Collaborative Infrastructure for Successful Astrobiology Research, Technology, and Education in Nevada.” A FORTRAN version of the FREZCHEM model is available from the senior author (GMM). We thank four reviewers and the Associate Editor (R.H. Byrne) for constructive comments and suggestions that improved the paper. We also thank Annette Risley for assistance in preparing the manuscript.

Associate editor: R. H. Byrne

REFERENCES

- Alpers C. N., Jambor J. L., and Nordstrom D. K. (eds.) (2000), Sulfate Minerals: Crystallography, Geochemistry, and Environmental Significance. Reviews in Mineralogy & Geochemistry, Vol. 40. Mineral. Soc. Am., Washington, DC.
- Banin A., Clark B. C., and Wänke H. (1992) Surface chemistry and mineralogy. In *Mars* (eds. H. H. Kieffer, C. W. Snyder, and M. S. Matthews). The University of Arizona Press, Tucson. pp. 594–625.
- Banin A., Han F.X., Kan I. and Cicelsky A. (1997) Acidic volatiles and the Mars soil. *J. Geophys. Res.* **102**, 13,341–13,356.
- Baird A. K. and Clark B. C. (1981) On the original igneous source of Martian fines. *Icarus* **45**, 113–123.
- Bernard A. and Symonds R. B. (1989) The significance of siderite in the sediments from Lake Nyos, Cameroon. *J. Volcanol. Geotherm. Res.* **39**, 187–194.
- Blaney D. L. and McCord T. B. (1989) An observational search for carbonates on Mars. *J. Geophys. Res.* **94**, 10,159–10,166.
- Bridges J. C., Catling D. C., Saxton J. M., Swindle T. D., Lyon I. C., and Grady M. M. (2001) Alteration assemblages in Martian meteorites: Implications for near-surface processes. *Space Sci. Rev.* **96**, 365–392.
- Bridges J. C. and Grady M. M. (2000) Evaporite mineral assemblages in the nakhlite (Martian) meteorites. *Earth Planet. Sci. Lett.* **176**, 267–280.
- Burns R. G. (1993) Rates and mechanisms of chemical weathering of ferromagnesian silicate minerals on Mars. *Geochim. Cosmochim. Acta* **57**, 4555–4574.
- Calvin W. M., King T. V., and Clark R. N. (1994) Hydrous carbonates on Mars? Evidence from Mariner infrared spectrometer and ground-based telescopic spectra. *J. Geophys. Res.* **99**, 14,659–14,675.
- Carr M. H. (1996) Water on Mars. Oxford University Press, New York.
- Catling D. C. (1999) A chemical model for evaporites on early Mars: Possible sedimentary tracers of the early climate and implications for exploration. *J. Geophys. Res.* **104**, 16,453–16,469.
- Catling D. C. and Moore J. (2000) Iron oxide deposition from aqueous solution and iron formations on Mars. *Lunar Planet. Sci. Conf. XXXI*. Lunar Planet. Inst., Houston.
- Christensen P. R., Anderson D. L., Chase S. C., Clancy R. T., Clark R. N., Conrath B. J., Kieffer H. H., Kuzmin R. O., Malin M. C., Pearl J. C., Roush T. L., and Smith M. D. (1998) Results from the Mars Global Surveyor Thermal Emission Spectrometer. *Sci.* **279**, 1,692–1,698.
- Christensen P. R., Bandfield J. L., Clark R. N., Edgett K. S., Hamilton V. E., Hoefen T., Kieffer H. H., Kuzmin R. O., Lane M. D., Malin M. C., Morris R. V., Pearl J. C., Pearson R., Roush T. L., Ruff S. W., and Smith M. D. (2000a) Detection of crystalline hematite mineralization on Mars by the Thermal Emission Spectrometer: Evidence for near-surface water. *J. Geophys. Res.* **105**, 9,623–9,642.
- Christensen P. R., Bandfield J. L., Smith M. D., Hamilton V. E., and Clark R. N. (2000b) Identification of a basaltic component on the Martian surface from Thermal Emission Spectrometer data. *J. Geophys. Res.* **105**, 9609–9621.
- Christensen P. R., Morris R. V., Lane M. D., Bandfield J. L., and Malin M. C. (2001) Global mapping of Martian hematite mineral deposits: Remnants of water-driven processes on early Mars. *J. Geophys. Res.* **106**, 23,873–23,885.
- Clark B. C. (1993) Geochemical components in Martian soil. *Geochim. Cosmochim. Acta* **57**, 4575–4581.
- Clark B. C. and Van Hart D. C. (1981) The salts of Mars. *Icarus* **45**, 370–378.
- Clegg S. L. and Brimblecombe P. (1990) The solubility and activity coefficient of oxygen in salt solutions and brines. *Geochim. Cosmochim. Acta* **54**, 3315–3328.
- Clegg S. L., Rard J. A., and Pitzer K. S. (1994) Thermodynamic properties of 0–6 mol kg⁻¹ aqueous sulfuric acid from 273.15 to 328.15 K. *Chem. Soc. Faraday Trans.* **90**, 1875–1894.
- Craig H. and Hayward T. (1987) Oxygen supersaturation in the ocean: Biological versus physical contributions. *Sci.* **235**, 199–202.
- Drever J. I. (1997) The Geochemistry of Natural Waters. Surface and Groundwater Environments. 3rd ed. Prentice-Hall, Upper Saddle River, New Jersey.
- Forget F. and Pierrehumbert R. T. (1997) Warming early Mars with carbon dioxide clouds that scatter infrared radiation. *Sci.* **278**, 1273–1276.
- Gaidos E. J. and Marion G. M. (2003) Geological and geochemical legacy of a cold early Mars. *J. Geophys. Res. Plan* **108**, No. E6, 5055.
- Garrels R. M. and Christ C. L. (1965) Solutions, Minerals, and Equilibria. Harper & Row, New York.
- Gooding J. L. (1992) Soil mineralogy and chemistry on Mars: Possible clues from salts and clays in SNC meteorites. *Icarus* **99**, 28–41.
- Griffith L. L. and Shock E. L. (1995) A geochemical model for the formation of hydrothermal carbonates on Mars. *Nature* **377**, 406–408.
- Haberle R. M. (1998) Early Mars climate models. *J. Geophys. Res.* **103**, 28,467–28,479.
- Harvie C. E., Møller N., and Weare J. H. (1984) The prediction of mineral solubilities in natural waters: The Na-K-Mg-Ca-H-Cl-SO₄-OH-HCO₃-CO₃-CO₂-H₂O system to high ionic strengths at 25°C. *Geochim. Cosmochim. Acta* **48**, 723–751.
- Head J. W. III, Kreslavsky M., Hiesinger H., Ivanov M., Pratt S., Seibert N., Smith D. E., and Zuber M. T. (1998) Oceans in the past history of Mars: Tests for their presence using Mars Orbiter Laser Altimeter (MOLA) data. *Geophys. Res. Lett.* **25**, 4401–4404.
- Kargel J. S. and Strom R. G. (1996) Global climatic change on Mars. *Sci. Am.* **275**, 80–88.
- Kasting J. F. (1991) CO₂ condensation and the climate of early Mars. *Icarus* **94**, 1–13.
- Kasting J. F. (1997) The early Mars climate question heats up. *Sci.* **278**, 1245.

- Kempe S. and Kazmierczak J. (1997) A terrestrial model for an alkaline Martian hydrosphere. *Planet. Space Sci.* **45**, 1493–1499.
- Kerr R. A. (2000) A wetter, younger Mars emerging. *Sci.* **289**, 714–716.
- Kieffer H. H., Jakosky B. M., and Snyder C. W. (1992) The planet Mars: From antiquity to the present. In *Mars* (eds. H. H. Kieffer, C. W. Snyder, and M. S. Matthews). The University of Arizona Press, Tucson, pp. 1–33.
- Königsberger E., Königsberger L.-C., and Gamsjäger H. (1999) Low-temperature thermodynamic model for the system $\text{Na}_2\text{CO}_3\text{-MgCO}_3\text{-CaCO}_3\text{-H}_2\text{O}$. *Geochim. Cosmochim. Acta* **63**, 3105–3119.
- Langmuir D. (1964) Thermodynamic properties of phases in the system $\text{CaO-MgO-CO}_2\text{-H}_2\text{O}$. *Geol. Soc. Am., Spec. Papers.* **82**, 120.
- Langmuir D. (1965) Stability of carbonates in the system $\text{MgO-CO}_2\text{-H}_2\text{O}$. *J. Geol.* **73**, 730–750.
- Lindsay W. L. (1979) *Chemical Equilibria in Soils*. John Wiley & Sons, New York.
- Linke W. F. (1958) *Solubilities of Inorganic and Metal Organic Compounds*. Vol. I. 4th ed. Am. Chem. Soc., Washington, DC.
- Lockwood J. P. and Rubin M. (1989) Origin and age of the Lake Nyos maar, Cameroon. *J. Volcanol. Geotherm. Res.* **39**, 117–124.
- Marion G. M. (2002) A molal-based model for strong acid chemistry at low temperatures (<200 to 298 K). *Geochim. Cosmochim. Acta* **66**, 2499–2516.
- Marion G. M. (2001) Carbonate mineral solubility at low temperatures in the $\text{Na-K-Mg-Ca-H-Cl-SO}_4\text{-OH-HCO}_3\text{-CO}_3\text{-CO}_2\text{-H}_2\text{O}$ system. *Geochim. Cosmochim. Acta* **65**, 1883–1896.
- Marion G. M. and Farren R. E. (1999) Mineral solubilities in the $\text{Na-K-Mg-Ca-Cl-SO}_4\text{-H}_2\text{O}$ system: A re-evaluation of the sulfate chemistry in the Spencer-Møller-Weare model. *Geochim. Cosmochim. Acta* **63**, 1305–1318.
- Marion G. M. and Grant S. A. (1994) FREZCHEM: A chemical-thermodynamic model for aqueous solutions at subzero temperatures. *CRREL Spec. Rept.* 94–18:USACRREL, Hanover, New Hampshire.
- Marion G. M., Schlesinger W. L., and Fonteyn P. J. (1985) CALDEP: A regional model for soil CaCO_3 (caliche) deposition in southwestern deserts. *Soil Sci.* **139**, 468–481.
- McKay C. P. and Stoker C. R. (1989) The early environment and its evolution on Mars: Implications for life. *Rev. Geophys.* **27**, 189–214.
- McSween H. Y. Jr. (1994) What we have learned about Mars from SNC meteorites. *Meteoritics* **29**, 757–779.
- McSween H. Y. Jr. and Murchie S. L. (1999) Rocks at the Mars Pathfinder landing site. *Am. Sci.* **87**, 36–45.
- Mironenko M. V., Grant S. A., Marion G. M., and Farren R. E. (1997) FREZCHEM2: A chemical thermodynamic model for electrolyte solutions at subzero temperatures. *CRREL Spec. Rept.*, 97–5:USACRREL, Hanover, New Hampshire.
- Morse J. W. and Marion G. M. (1999) The role of carbonates in the evolution of early Martian oceans. *Am. J. Sci.* **299**, 738–761.
- Newsom H. E. (1996) Martians in a deep freeze. *Nature* **379**, 205–206.
- Nordstrom D. K., Plummer L. N., Langmuir D., Busenberg E., May H. M., Jones B. F., and Parkhurst D. L. (1990) Revised chemical equilibrium data for major water-mineral reactions and their limitations. In *Chemical Modeling of Aqueous Systems II* (eds. C. Melchior and R.L. Bassett) pp. 398–413. ACS Symposium Series 416.
- Pitzer K. S. (1991) Ion interaction approach: Theory and data correlation. In *Activity Coefficients in Electrolyte Solutions, 2nd ed.* (ed. K. S. Pitzer) pp. 75–153. CRC Press, Boca Raton.
- Pitzer K. S. (1995) *Thermodynamics*, 3rd ed. McGraw-Hill, New York.
- Plummer L. N., Parkhurst D. L., Fleming G. W., and Dunkle S. A. (1988) A computer program incorporating Pitzer's equations for calculation of geochemical reactions in brines. *U. S. Geol. Surv. Water Res. Inv. Rep.* 88–4153.
- Pollack J. B., Roush T., Witteborn F., Bregman J., Wooden D., Stoker C., Toon O. B., Rank D., Dalton B., and Freedman R. (1990) Thermal emission spectra of Mars (5.4–10.5 μm): Evidence for sulfates, carbonates, and hydrates. *J. Geophys. Res.* **95**, 14,595–14,627.
- Ptacek C. J. (1992) Experimental determination of siderite solubility in high ionic-strength aqueous solutions. Ph.D. thesis, University of Waterloo, Ontario, Canada.
- Ptacek C. J. and Blowes D. W. (1994) Influence of siderite on the pore-water chemistry of inactive mine-tailings impoundments. In *Environmental Geochemistry of Sulfide Oxidation* (eds. C.N. Alpers and D.W. Blowes). Am. Chem. Soc. Symp. Ser. **550**, 172–180.
- Ptacek C. J. and Blowes D. W. (2000) Predicting sulfate-mineral solubility in concentrated waters. In *Sulfate Minerals: Crystallography, Geochemistry, and Environmental Significance*, (eds. C. N. Alpers, J. L. Jambor, and D. K. Nordstrom). Reviews in Mineralogy & Geochemistry, Vol. 40, pp. 513–540. Mineral. Soc. Am., Washington, DC.
- Reardon E. J. and Beckie R. D. (1987) Modelling chemical equilibria of acid mine-drainage: The $\text{FeSO}_4\text{-H}_2\text{SO}_4\text{-H}_2\text{O}$ system. *Geochim. Cosmochim. Acta* **51**, 2355–2368.
- Reed M. H. (1982) Calculation of multicomponent chemical equilibria and reaction processes in systems involving minerals, gases and an aqueous phase. *Geochim. Cosmochim. Acta* **46**, 513–528.
- Reed M. H. and Spycher N. (1984) Calculation of pH and mineral equilibria in hydrothermal waters with application to geothermometry and studies of boiling and dilution. *Geochim. Cosmochim. Acta* **48**, 1479–1492.
- Rieder R., Economou T., Wänke H., Turkevich A., Crisp J., Brückner J., Dreibus G., and McSween H. Y. Jr. (1997) The chemical composition of Martian soil and rocks returned by the Mobile Alpha Proton X-ray Spectrometer: Preliminary results from the X-ray mode. *Sci.* **278**, 1771–1774.
- Sagan C. and Chyba C. (1997) The early faint sun paradox: Organic shielding of ultraviolet-labile greenhouse gases. *Sci.* **276**, 1217–1221.
- Schäfer H. (1949) Dampfdruck- und Löslichkeitsmessungen an Eisen(II)-chlorid-hydraten. *Z. Anorg. Chem.* **258**, 69–76.
- Schaefer M. W. (1990) Geochemical evolution of the Northern Plains of Mars: Early hydrosphere, carbonate development, and present morphology. *J. Geophys. Res.* **95**, 14,291–14,300.
- Schaefer M. W. (1993) Aqueous geochemistry of early Mars. *Geochim. Cosmochim. Acta* **57**, 4619–4625.
- Schimmel F. A. (1952) The ternary systems: Ferrous chloride-hydrogen chloride-water, ferric chloride-ferrous chloride-water. *J. Am. Chem. Soc.* **74**, 4689–4691.
- Settle M. (1979) Formation and deposition of volcanic sulfate aerosols. *J. Geophys. Res.* **84**, 8343–8354.
- Spencer R. J., Möller N., and Weare J. H. (1990) The prediction of mineral solubilities in natural waters: A chemical equilibrium model for the $\text{Na-K-Ca-Mg-Cl-SO}_4\text{-H}_2\text{O}$ system at temperatures below 25°C. *Geochim. Cosmochim. Acta* **54**, 575–590.
- Toulmin P. III, Baird A. K., Clark B. C., Keil K., Rose H. J. Jr., Christian R. P., Evans P. H., and Kelliher W. C. (1977) Geochemical and mineralogical interpretation of the Viking inorganic chemical results. *J. Geophys. Res.* **82**, 4625–4634.
- Zent A. P. (1996) The evolution of the Martian climate. *Am. Sci.* **84**, 442–451.